A HYPERBOLIC 4-MANIFOLD WITH A PERFECT CIRCLE-VALUED MORSE FUNCTION

LUDOVICO BATTISTA AND BRUNO MARTELLI

Abstract. We exhibit a finite-volume cusped hyperbolic four-manifold W with a perfect circle-valued Morse function, that is a circle-valued Morse smooth function $f\colon W \to S^1$ with $\chi(W)$ critical points, all of index 2. The map f is built by extending and smoothening a combinatorial Morse function defined by Jankiewicz – Norin – Wise [14] via Bestvina – Brady theory [4].

By elaborating on this construction we also prove the following facts:

- There are infinitely many finite-volume hyperbolic 4-manifolds M having a handle decomposition with bounded numbers of 1- and 3-handles, so with bounded Betti numbers $b_1(M), b_3(M)$ and rank $\mathrm{rk}(\pi_1(M))$.
- The kernel of $f_*\colon \pi_1(W) \to \pi_1(S^1) = \mathbb{Z}$ determines a geometrically infinite hyperbolic four-manifold $\widetilde{W}$ obtained by adding infinitely many 2-handles to a product $N \times [0,1]$, for some cusped hyperbolic 3-manifold N. The manifold $\widetilde{W}$ is infinitesimally (and hence locally) rigid.
- There are type-preserving representations of the fundamental groups of `m036` and of the surface Σ with genus 2 and one puncture in $\mathrm{Isom}^+(\mathbb{H}^4)$ whose image is a discrete subgroup with limit set S^3. These representations are not faithful. We do not know if they are rigid.

Introduction

One of the most intriguing phenomena in 3-dimensional topology is the existence of many finite-volume hyperbolic 3-manifolds M that fiber over S^1. On such manifolds, the surface fiber Σ generates a normal subgroup $\pi_1(\Sigma) \lhd \pi_1(M)$ and determines a geometrically infinite covering $\widetilde{M} \to M$ diffeomorphic to $\Sigma \times \mathbb{R}$. Every finite-volume hyperbolic 3-manifold is finitely covered by a 3-manifold that fibers over S^1 by a celebrated theorem of Agol and Wise [1, 30]. All the hyperbolic manifolds and orbifolds in this paper are tacitly assumed to be complete.

We could ask whether such fibrations occur also in higher dimension $n \geq 4$. The answer is certainly negative in even dimensions, for a simple reason: by the generalised Gauss – Bonnet formula, the Euler characteristic of an even-dimensional finite-volume hyperbolic manifold does not vanish, while that of a fibration does.

The following seems a more sensible question to ask.

Question 1. Are there finite-volume hyperbolic n-manifolds with perfect circle-valued Morse functions in all dimensions n?

Unless otherwise stated, all the manifolds N in this introduction are without boundary, and they are either compact or diffeomorphic to the interior of a compact manifold with boundary that we denote by N^*. As a consequence of the Margulis Lemma, every finite-volume hyperbolic n-manifold is of this type.

A circle-valued Morse function on a manifold M is a smooth map $f\colon M \to S^1$ with only finitely many critical points, all of non degenerate type. If M is not itself compact, by our assumption it is diffeomorphic to the interior of a compact M^* with boundary and in this case we also require f to extend to a circle-valued Morse function on M^* with no critical points on ∂M^*. So the restriction of f to some collar of ∂M^* is a fibration and all the critical points lie in the interior of M^*. This condition is quite restrictive, since it implies that $f|_{\partial M^*}$ is a fibration.

A circle-valued Morse function $f\colon M \to S^1$ is *perfect* if it has exactly $|\chi(M)|$ critical points. In general we have

$$\chi(M) = \sum (-1)^i c_i$$

where c_i is the number of critical points of index i. Therefore f is perfect if and only if it has the minimum possible number of critical points allowed by $\chi(M)$.

In odd dimensions we have $\chi(M) = 0$ and hence a perfect circle-valued Morse function is just a fibration. In dimension 2, every closed orientable surface has a perfect circle-valued Morse function. In dimension 4, a finite-volume hyperbolic four-manifold M has $\chi(M) > 0$ and a circle-valued Morse function on M is perfect if and only if all the critical points have index 2. Our main contribution is to provide and study a first example.

Theorem 2. *The finite-volume cusped hyperbolic 4-manifold W with 24 cusps and $\chi(W) = 8$ defined in* [20, 23] *has a perfect circle-valued Morse function $f\colon W \to S^1$.*

The manifold W was built in [20, 23] by assembling eight ideal 24-cells along a very symmetric cubic pattern. It has 24 cusps, each with a 3-torus section. By assumption, the function f extends to the compact W^* and is a fibration on each of the 24 boundary 3-tori of W^*.

We construct $f\colon W \to S^1$ by extending and smoothening a combinatorial Morse function defined in a recent very nice paper of Jankiewicz – Norin – Wise [14] via Bestvina – Brady theory [4]. The fact that this smoothening produces only critical points of index 2 is due to the extraordinary nice features of the 24-cell. In particular we will use that its vertices form the binary tetrahedral group in quaternions space.

The regular and singular fibers. Our main goal is to try to visualize $f\colon W \to S^1$ and to study and understand its topological properties.

We represent the perfect Morse function $f\colon W \to S^1$ quite sketchy in Figure 1. We identify S^1 with $\mathbb{R}/_{2\mathbb{Z}}$. There are two critical values 0 and 1, each having four critical points in its counterimage. In principle, there should be four homeomorphism types of fibers: two singular ones $f^{-1}(0)$ and $f^{-1}(1)$ and two regular ones

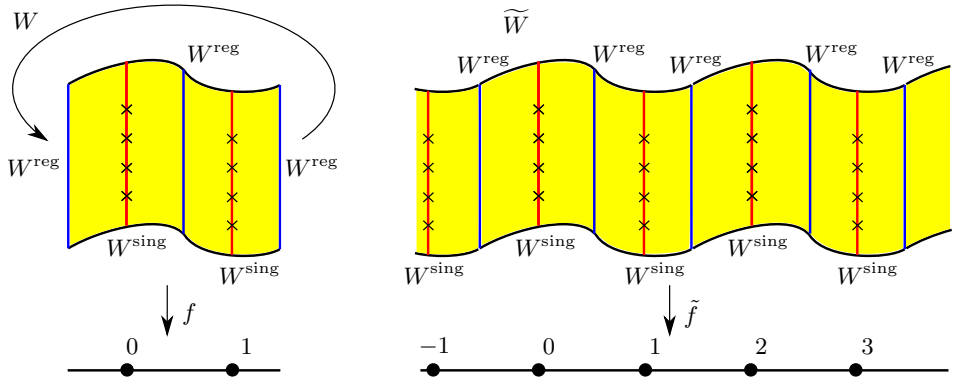

FIGURE 1. The circle-valued Morse function $f\colon W \to S^1$ (left) and its lift $\tilde{f}\colon \widetilde{W} \to \mathbb{R}$ (right). There are two critical values 0 and 1 for f, each containing 4 critical points in its counterimage, indicated with an X. The function f has two homeomorphism types of fibers, the regular one W^{reg} and the singular one W^{sing} that contains 4 critical points. The function $\tilde{f}$ has the same types of fibers, repeated infinitely many times.

$f^{-1}\big(\pm\frac{1}{2}\big)$, but these actually reduce to two since the pairs of singular and regular fibers turn out to be homeomorphic.

The regular fiber $W^{\mathrm{reg}} = f^{-1}\big(\pm\frac{1}{2}\big)$ is a hyperbolic 3-manifold with volume ~ 152.510077 and 24 cusps, each contained in a cusp of W. It may be identified as the double cover of the (quite messy) orbifold O shown in Figure 2. The orbifold O is tessellated into 24 (non regular) ideal octahedra (precisely as the boundary of the 24-cell), and W^{reg} into 48.

The singular fiber $W^{\mathrm{sing}} = f^{-1}(0) = f^{-1}(1)$ contains 4 critical points. If we remove the 4 critical points from W^{sing} we get a hyperbolic 3-manifold $\mathring{W}^{\mathrm{sing}}$ with volume ~ 194.868788 and 28 cusps. It decomposes nicely into 192 regular ideal tetrahedra. The singular fiber W^{sing} is obtained by coning 4 of these 28 cusps.

The regular fiber $f^{-1}(\pm\varepsilon)$ is obtained from the singular fiber $f^{-1}(0)$ by substituting the four critical points with four circles, that is by Dehn filling. Since the regular fibers $f^{-1}(\pm\varepsilon)$ are both homeomorphic to W^{reg}, the manifold W^{reg} is obtained by Dehn filling 4 cusps of $\mathring{W}^{\mathrm{sing}}$ in two different ways. This 3-dimensional phenomenon is called *cosmetic Dehn filling* [5].

The appearance of regular ideal tetrahedra in this context is quite unexpected and is due (again) to the many nice properties of the 24-cell.

Like in the more familiar fibrations in dimension 3, the fibers W^{reg} and W^{sing} are embedded in W in a very pleated way: they are decomposed respectively into geometric octahedra and tetrahedra that form some angles along their 2-dimensional

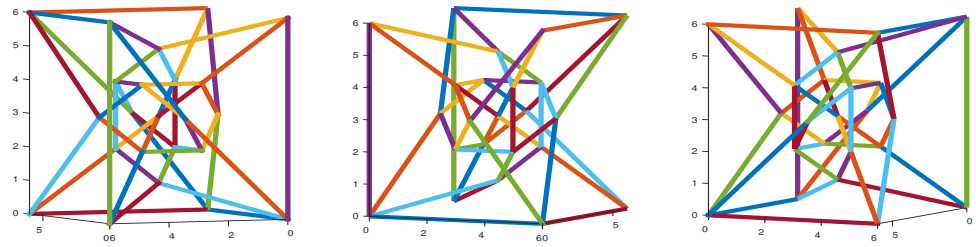

FIGURE 2. The hyperbolic orbifold O has base space S^3 (with 24 punctures) and singular locus the (quite complicated) knotted 4-valent graph shown here with respect to three different viewpoints. The graph has 24 vertices that should be removed and indicate 24 cusps, each based on the flat orbifold $(S^2, 2, 2, 2, 2)$. For the sake of clarity, we omit the vertex at infinity and four edges that are connected to it. The graph is contained in the 1-skeleton of the 24-cell. It has many symmetries that are unfortunately not apparent from the figure.

faces, in such a complicated way that any connected component X of the preimage of W^{reg} or W^{sing} in $\mathbb{H}^4$ has the whole sphere at infinity $S^3 = \partial\mathbb{H}^4$ as a limit set.

A crucial difference with the fibrations that one encounters in dimension 3 is that the fibers W^{reg} and W^{sing} are not π_1-injective in W, because the index-2 critical points kill some of the elements in their fundamental groups. This implies that the connected component X just mentioned is not simply connected.

These phenomena may be better understood by looking at the abelian cover $\widetilde{W}$.

The geometrically infinite manifold $\widetilde{W}$. The kernel of $f_*\colon \pi_1(W) \to \pi_1(S^1) = \mathbb{Z}$ determines a covering $\widetilde{W} \to W$ and a lift $\tilde{f}\colon \widetilde{W} \to \mathbb{R}$ as in Figure 1. The regular fiber W^{reg} lifts to $\widetilde{W}$, and $\widetilde{W}$ is diffeomorphic to $W^{\text{reg}} \times [0, 1]$ with infinitely many 2-handles attached on both sides. In particular the induced map $\pi_1(W^{\text{reg}}) \to \pi_1(\widetilde{W})$ is surjective and hence $\pi_1(\widetilde{W})$ is finitely generated. However, it is not injective. We will soon see that $\pi_1(\widetilde{W})$ cannot be finitely presented.

Since $\pi_1(\widetilde{W})$ is normal in $\pi_1(W)$ and W has finite volume, the limit set of $\widetilde{W}$ is the whole sphere at infinity $S^3 = \partial\mathbb{H}^4$. In particular the manifold $\widetilde{W}$ is geometrically infinite and its topology and geometry are worth being studied. We can show the following.

Theorem 3. *The hyperbolic manifold $\widetilde{W}$ has 24 cusps, each with section diffeomorphic to $S^1 \times S^1 \times \mathbb{R}$. Its Betti numbers are*

$$b_1(\widetilde{W}) = 20, \qquad b_2(\widetilde{W}) = \infty, \qquad b_i(\widetilde{W}) = 0 \ \forall i \geq 3.$$

The holonomy representation of $\widetilde{W}$ is infinitesimally (and hence locally) rigid.

The fundamental group of $\widetilde{W}$ is finitely generated, but since $b_2(\widetilde{W}) = \infty$ it cannot be finitely presented.

The infinitesimal rigidity of $\widetilde{W}$ is in contrast to dimension three, where as a consequence of the (now proved [6, 7, 26]) density conjecture we know that every geometrically infinite 3-manifold can be deformed into a geometrically finite one. As a general fact, experiencing more rigidity in dimension $n \geq 4$ should not be much of a surprise, especially for a manifold that has infinitely many 2-handles.

To the best of our knowledge, the manifold $\widetilde{W}$ is the first example of a rigid geometrically infinite hyperbolic manifold in any dimension.

A smaller example. The manifolds W and $\widetilde{W}$ have plenty of symmetries, that we study carefully here. SnapPy tells us that the isometry group of W^{reg} has order 192. These facts suggest that it might be possible to find some examples of perfect Morse functions on some hyperbolic 4-manifold smaller than W by quotienting $\widetilde{W}$ along some appropriate group of isometries. This is the case.

The smallest interesting example that we have found is a hyperbolic 4-orbifold Y with only one isolated singularity p having a lens space as a link. We pay the price of accepting this very mild kind of singularity, and as a reward be get some very small 4-orbifold whose topology we can fully understand.

We reassure the reader that it makes perfectly sense to talk about Morse functions with only index-2 critical points on 4-orbifolds with isolated singularities based on lens spaces. A Morse function f near an index-2 critical point is equivalent to $f(x_1, x_2, x_3, x_4) = x_1^2 + x_2^2 - x_3^2 - x_4^2$. Such a function f is $\mathrm{SO}(2) \times \mathrm{SO}(2)$-invariant and hence descends to a function on the cone over any lens space.

Theorem 4. *There is a finite-volume hyperbolic 4-orbifold Y with $\chi(Y) = \frac{1}{12}$ whose singular set is a single point p with link the lens space $L(12, 5)$, equipped with a circle-valued Morse function $f\colon Y \to S^1$ with a single index-2 critical point at p. The orbifold Y has a single cusp with section a flat torus bundle over S^1.*

The regular fiber Y^{reg} of f is the manifold `m036` *from the census* [8]*, while the singular fiber Y^{sing} is the complement of the link in Figure 3 with one cusp coned.*

If we compare W and Y, we note that Y is 96 times smaller than W, it has only one cusp (whereas W has 24), the circular Morse function f has only one singular point (while that of W has 8), and the regular and singular fibers of Y are 48 times smaller than those of W. The fibers are in fact so small that they appear among the first hyperbolic manifolds in the census [8].

The hyperbolic manifold $Y^{\mathrm{reg}} =$ `m036` has one cusp, volume ~ 3.177293, and homology $\mathbb{Z} \times \mathbb{Z}_3$. It decomposes into a non-regular ideal octahedron [11]. The complement $\mathring{Y}^{\mathrm{sing}}$ of the link `L6a2` shown in Figure 3 is the hyperbolic manifold `m203`; it has volume ~ 4.059766 and decomposes into four regular ideal tetrahedra [8]. The manifolds Y^{reg} and $\mathring{Y}^{\mathrm{sing}}$ are covered by W^{reg} and $\mathring{W}^{\mathrm{sing}}$.

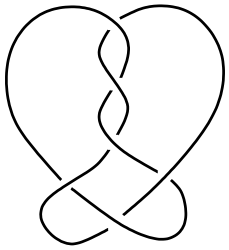

FIGURE 3. The link L6a2 from Thistelthwaite's link table. Its complement is the hyperbolic manifold m203. If we cone one cusp of $\mathring{Y}^{\text{sing}} = \texttt{m203}$ we get the singular fiber Y^{sing} of a circle-valued Morse function $f\colon Y \to S^1$ with one critical point p on a 4-dimensional hyperbolic orbifold Y.

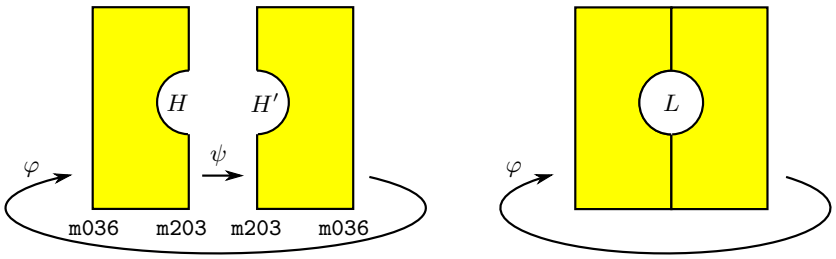

FIGURE 4. The orbifold Y is constructed by assembling two copies of the same yellow block via the isometries φ and ψ, and then filling the hole by coning the resulting boundary component homeomorphic to $H \cup H' = L = L(12,5)$.

We can now furnish a quite satisfactory topological description of Y. We employ the usual meridian-longitude basis of Figure 3. Using SnapPy [9] we discover that if we Dehn fill one cusp of m203 by killing the slope $\pm\frac{3}{2}$ we get m036. It is not necessary to specify which component of the link is filled since they are symmetric. SnapPy also says that there is an isometry ψ of m203 that sends the slope $\frac{r}{s}$ to $-\frac{r}{s}$, and this explains why we get the same manifold m036 by killing the slope $\pm\frac{3}{2}$. Using SnapPy we also discover the following fundamental fact: the filled manifold m036 has an *additional isometry* φ that is not induced from m203.

Topologically, the manifold Y may be visualized as in Figure 4. Let $K \subset \texttt{m036}$ be the knot whose complement is m203. The *yellow block* in the figure is the manifold $\texttt{m036} \times [0,1]$, with a small tubular neighbourhood of $K \times \{1\}$ removed. The yellow block is homeomorphic to $\texttt{m036} \times [0,1]$ but it should be interpreted as a manifold with corners; it has a left boundary component $\texttt{m036} \times \{0\}$ and a right boundary component that consists of two parts: these are $\texttt{m203} \subset \texttt{m036} \times \{1\}$ and a solid torus $H \subset \texttt{m036} \times (0,1]$, attached along a corner torus ∂H. Both the left and boundary

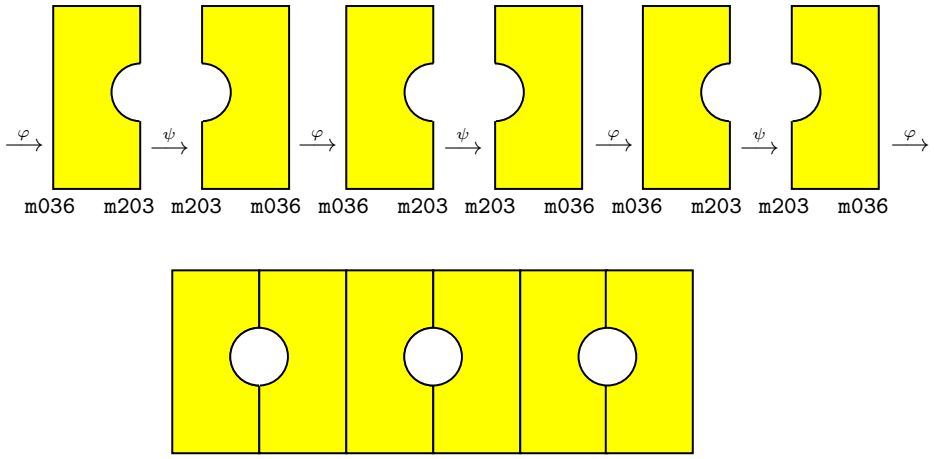

FIGURE 5. The geometrically infinite orbifold $\tilde{Y}$ is constructed by assembling infinitely many copies of the same yellow block via the isometries φ, ψ, and then coning the resulting holes, each diffeomorphic to $L(12,5)$.

components are homeomorphic to `m036`, but the right one is cornered along the torus.

The orbifold Y is constructed by assembling two identical yellow blocks as in Figure 4, using the isometries ψ and φ as gluing maps. The gluing produces a 4-manifold with one boundary component (represented as a circle in the figure), which is the union of the two solid tori H and H' of the two yellow blocks. The meridians of H and H' are $\binom{3}{2}$ and $\binom{-3}{2}$, so the two solid tori give rise to the lens space $L(12,5)$. Finally, we cone this lens space boundary component, thus producing a singular point. The result is Y.

Remark 5. To the best of our knowledge, the orbifold Y is the first example of a finite-volume hyperbolic orientable 4-orbifold with the smallest possible type of singularity, namely a single point. It decomposes into two pyramids with octahedral base, see Section 5.6.

In some embarrassingly vague sense, the two isometries ψ and φ look like the matrices $\left(\begin{smallmatrix}1&1\\0&1\end{smallmatrix}\right)$ and $\left(\begin{smallmatrix}1&0\\1&1\end{smallmatrix}\right)$, that when multiplied give rise to the Anosov $\left(\begin{smallmatrix}2&1\\1&1\end{smallmatrix}\right)$, the monodromy of the famous fibration of the figure-8 knot complement.

Remark 6. It is crucial here that φ is an additional isometry, that is it does not preserve `m203`. If φ preserved `m203`, the map $f\colon Y \to S^1$ would restrict to a fibration with fiber `m203`, which is virtually trivial (because the isometries of `m203` form a finite group), and this would easily produce many non-peripheral subgroups $\mathbb{Z} \times \mathbb{Z} < \pi_1(Y)$, forbidding Y to be hyperbolic. This would be analogous to a reducible monodromy in dimension three.

An explicit geometrically infinite Klenian group with 2 generators. As above, the Morse function $f\colon Y \to S^1$ induces a homomorphism $f_*\colon \pi_1(Y) \to \pi_1(S^1) = \mathbb{Z}$ with finitely generated kernel, that yields a geometrically infinite orbifold $\tilde{Y}$ covering Y and a lifted Morse function $\tilde{f}\colon \widetilde{Y} \to \mathbb{R}$ with only index-2 critical points. The orbifold $\tilde{Y}$ has infinitely many singular points and its topology can be visualized as in Figure 5, as the attachment of infinitely many identical yellow blocks, and the subsequent coning of infinitely many lens space boundaries. This topological description is somehow reminiscent of Minsky's model manifold decomposition into blocks [24].

We stress that the fundamental group $\pi_1(\tilde{Y})$ is finitely generated, although $\widetilde{Y}$ has infinitely many singular points: the existence of Kleinian groups in dimension 4 with infinitely many conjugacy classes of finite subgroups is not a surprise [16]. The orbifold $\tilde{Y}$ has only one cusp, with section diffeomorphic to $S^1 \times S^1 \times \mathbb{R}$.

We can describe explicitly some generators for $\pi_1(\tilde{Y})$ and their holonomies. We discover in particular that $\pi_1(\tilde{Y})$ can be generated by two elements. The regular fiber $Y^{\mathrm{reg}} = \mathtt{m036}$ of $\tilde{Y}$ induces a surjective homomorphism $i_*\colon \pi_1(\mathtt{m036}) \to \pi_1(\tilde{Y})$. By composing it with the holonomy of $\tilde{Y}$ we get a representation

$$\Phi\colon \pi_1(\mathtt{m036}) \longrightarrow \mathrm{Isom}^+(\mathbb{H}^4) = \mathrm{SO}^+(4,1)$$

whose image is a geometrically infinite discrete group Γ such that $\tilde{Y} = \mathbb{H}^4/_\Gamma$. The representation Φ is not injective. We can write everything explicitly.

Theorem 7. *A presentation for* $\pi_1(\mathtt{m036})$ *is*

$$\langle\ a, b \mid a^{-2}b^{-2}ab^{-2}a^{-2}b\ \rangle.$$

We have

$$\Phi(a) = \begin{pmatrix} 1/2 & -1/2 & 1/2 & 1/2 & 0 \\ 1/2 & 1/2 & -1/2 & 1/2 & 0 \\ 1/2 & -1/2 & -1/2 & -1/2 & 0 \\ 1/2 & 1/2 & 1/2 & -1/2 & 0 \\ 0 & 0 & 0 & 0 & 1 \end{pmatrix},$$

$$\Phi(b) = \begin{pmatrix} -7/2 & 3/2 & 3/2 & 3/2 & 3\sqrt{2} \\ -3/2 & 1/2 & 1/2 & -1/2 & \sqrt{2} \\ 3/2 & 1/2 & -1/2 & -1/2 & -\sqrt{2} \\ 3/2 & -1/2 & 1/2 & -1/2 & -\sqrt{2} \\ -3\sqrt{2} & \sqrt{2} & \sqrt{2} & \sqrt{2} & 5 \end{pmatrix}.$$

Both $\Phi(a)$ and $\Phi(b)$ are elliptic of order 12, while a and b have infinite order in $\pi_1(\mathtt{m036})$. By construction the representation Φ is *type-preserving*, that is it sends parabolics to parabolics. The geometrically infinite group Γ has only two generators and these are expressed explicitly above as some elliptic transformations. The limit set of Γ is the whole sphere at infinity $S^3 = \partial\mathbb{H}^4$.

We can descend one dimension further: we discover from [3] that `m036` fibers over S^1 with fiber the surface Σ with genus 2 and one puncture. We deduce the following.

Corollary 8. *There is a type-preserving representation $\Phi\colon \pi_1(\Sigma) \to \mathrm{Isom}(\mathbb{H}^4)$ whose image is a discrete geometrically infinite group with limit set $S^3 = \partial\mathbb{H}^4$.*

Proof. We have $\pi_1(\Sigma) \lhd \pi_1(\texttt{m036})$. Since $\Phi\colon \pi_1(\texttt{m036}) \to \Gamma$ is surjective, the image $\Phi(\pi_1(\Sigma))$ is normal in Γ, which is in turn normal in the holonomy group Γ' of the finite-volume orbifold Y . Therefore

$$\Lambda(\Phi(\pi_1(\Sigma)) = \Lambda(\Gamma) = \Lambda(\Gamma') = S^3.$$

The proof is complete. □

Question 9. Can we deform type-preservingly the representations Φ of $\pi_1(\texttt{m036})$ and $\pi_1(\Sigma)$? Can we find a path connecting them to their Fuchsian representations, or to any geometrically finite discrete representation?

Infinitely many hyperbolic 4-manifolds with bounded invariants. Using Theorem 2 we may easily construct infinitely many finite-volume hyperbolic 4-manifolds that can be represented via a handle decomposition with a bounded number of 1- and 3-handles.

Corollary 10. *There is a $K > 0$ and there are infinitely many pairwise non-homeomorphic finite-volume hyperbolic 4-manifolds $M_1, M_2, \dots$ such that each M_j^* has a handle decomposition with at most K i-handles for all $i \neq 2$.*

Proof. Pick the perfect Morse function $f\colon W \to S^1$ of Theorem 2. It has $\chi(W) = 8$ critical points of index 2. The fiber of a regular value is a compact 3-manifold W^{reg}. Fix a handle decomposition of $(W^{\mathrm{reg}})^*$ with some g_i distinct i-handles for $i = 0, 1, 2, 3$. By thickening it and adding new handles to fill W^* we easily get a handle decomposition for W^* with g_0 zero-handles, $g_0 + g_1$ one-handles, $g_1 + g_2 + \chi(W)$ two-handles, $g_2 + g_3$ three-handles, and g_3 four-handles.

For every natural number $n \geq 1$ we may consider the degree-n covering $W_n \to W$ induced by the kernel of $\pi_1(W) \to \pi_1(S^1) = \mathbb{Z} \to \mathbb{Z}_n$. The composed Morse function $W_n \to W \to S^1$ has the same regular fiber W^{reg} considered above and $\chi(W_n) = n\chi(W) = 8n$ critical points of index 2. The induced handle decomposition of W_n^* has the same number of i-handles as that of W^*, except for $i = 2$. The sequence $W_1, W_2, \dots$ of hyperbolic manifolds fulfills the requirements of the theorem. □

The following corollary seems also new.

Corollary 11. *There are infinitely many finite-volume hyperbolic 4-manifolds M with bounded Betti numbers $b^i(M) < K$ for all $i \neq 2$, and also with bounded rank $\mathrm{rk}(\pi_1(M)) < K$.*

These results cannot be extended to $i = 2$, since $\chi(M) \leq 2 + b_2(M)$ and there are only finitely many finite-volume hyperbolic 4-manifolds M up to isometry with bounded $\chi(M)$ by a theorem of Wang [28].

Related results and further research. The first explicit example of a geometrically infinite Γ was built by Jørgensen [15] in dimension 3. Geometrically infinite hyperbolic 3-manifolds have been studied intensively since then and they are now quite well understood; the higher dimensional ones are much more mysterious: see [17, Problem 2.10], where the construction of a geometrically infinite hyperbolic manifold of dimension $n \geq 4$ that is not derived from a 3-dimensional example is stated as an open problem.

The recent papers [14] and [2] provide some new constructions in dimension 4. In both papers it is shown that some lattices $\Gamma < \mathrm{Isom}(\mathbb{H}^4)$ *fiber algebraically*, that is they have an epimorphism $g\colon \Gamma \to \mathbb{Z}$ with finitely generated kernel. The kernel $\Gamma' = \ker g$ is geometrically infinite. More instruments to produce algebraic fibrations via the RFRS condition were designed by Friedl – Vidussi [10] and Kielak [18]. More examples of hyperbolic manifolds in dimension up to 8 are constructed in [13].

In general an algebraic fibration does not produce a nice circle-valued Morse smooth function. As we mentioned above, the construction here is facilitated by the exceptional features of the 24-cell. It would be interesting to have more examples in dimension 4, in other commensurability classes. We raise in particular the following.

Question 12. Is there a compact hyperbolic 4-manifold with a perfect Morse function?

The techniques introduced in this paper apply to the ideal right-angled 24-cell, but not to the compact right-angled 120-cell, because it is too big: see Remark 23. On the other hand, we note that if M has a perfect Morse function then all its finite coverings also have. It therefore makes sense to ask the following.

Question 13. Does every finite-volume hyperbolic 4-manifold virtually have a perfect Morse function? Equivalently, is there one such manifold in every commensurability class?

Concerning rigidity:

Question 14. Is every geometrically infinite manifold constructed from an algebraic fibration (or a perfect Morse function) rigid in dimension $n \geq 4$?

We mention that every compact hyperbolic n-manifold with geodesic boundary is rigid [19] when $n \geq 4$.

Structure of the paper. The paper is organized as follows. The first three chapters introduce the main tools, that can be applied on any right-angled polytope P in $\mathbb{H}^n, \mathbb{R}^n$, or S^n to construct manifolds M tessellated by some copies of P and circle-valued functions $M \to S^1$: these are the *colourings* (already used by various authors), the *diagonal maps* (from Bestvina – Brady [4]), and the *states* (from Jankiewicz – Norin – Wise [14]).

These tools are used to construct the manifold W and the circle-valued Morse function $W \to S^1$, which is then studied in Chapter 4. The quotient orbifold $Y \to S^1$ is then introduced and investigated in Chapter 5. Finally, the rigidity of $\widetilde{W}$ is proved in Section 6.

Acknowledgements. We thank Marc Culler and Matthias Goerner for helpful discussions.

1. Colourings

1.1. **Right-angled polytopes.** Let $P \subset \mathbb{X}^n$ be a right-angled finite polytope in some space $\mathbb{X}^n = \mathbb{H}^n, \mathbb{R}^n$ or $\mathbb{S}^n$. Let $\Gamma < \mathrm{Isom}(\mathbb{X}^n)$ be the group generated by the reflections along the facets of P. It is a standard nice fact about Coxeter polytopes that P is a fundamental domain for the action of Γ, and a presentation of Γ is

$$\langle\, r_1, \dots, r_s \mid r_i^2, [r_i, r_j] \,\rangle.$$

Here r_i is the reflection along the i-th facet of P and the relation $[r_i, r_j] = 0$ occurs whenever the i-th and j-th facet are adjacent. We may also consider P as an orbifold $P = \mathbb{X}^n/\Gamma$.

Here we will always suppose that P has finite volume. We are of course mostly interested in the hyperbolic geometry $\mathbb{X}^n = \mathbb{H}^n$, where P may or may not have ideal vertices.

1.2. **Colours.** Let $P \subset \mathbb{X}^n$ be a right-angled finite polytope. We may easily construct some manifold cover $M \to P$ by colouring its facets. This is a standard procedure that was used for instance in [20].

A *colouring* of P is the assignment of a colour (taken from some finite set) to each facet of P, such that incident facets have distinct colours. We use $\{1, \dots, c\}$ as a palette of colours and suppose that every colour is painted on at least one facet.

A colouring induces a map $\Gamma \to \mathbb{Z}_2^c$ that sends r_i to e_j, where j is the colour assigned to the i-th facet of P. One verifies that the kernel $\Gamma' \lhd \Gamma$ acts freely on $\mathbb{X}^n$ and hence we get a manifold $M = \mathbb{X}^n/\Gamma'$ that orbifold-covers $P = \mathbb{X}^n/\Gamma$ with degree 2^c. The manifold M is tessellated into 2^c copies of P.

Geometrically, we may see M as constructed by mirroring P iteratively along its colours, in any order. More formally, consider 2^c copies of P denoted as P^v where $v \in \mathbb{Z}_2^c$ varies. The facet F of P^v is identified via the identity map to the same facet of P^{v+e_j} whenever F il coloured by j.

1.3. **The dual cube complex.** If a manifold M is tessellated into finitely many right-angled polytopes, we dually get a finite cube complex $C \subset M$ topologically embedded in M (we indicate with the letter C both the cube complex and its support, for simplicity). We may define $C \subset M$ in the piecewise-linear category as a union of simplexes in the barycentric subdivision of the polytopes.

If P is compact, then M also is and $C = M$. If $P \subset \mathbb{H}^n$ has some ideal vertices, then M is cusped and hence diffeomorphic to the interior of a compact manifold M^*, whose boundary consists of some flat closed $(n-1)$-manifolds. In this case $C \subset M^*$ is a proper subset onto which M^* collapses (a spine of M^*), and $M^* \setminus C$ is homeomorphic to $\partial M^* \times [0,1)$. If needed we can easily extend C to a cube complex C^* with $M^* = C^*$ as follows. (We mainly use C and see C^* only as a technical modification, so this construction can be skipped at first reading.)

We use a cusp section of M to truncate simultaneously all the polytopes of the tessellation at their ideal vertices. In such a way we obtain a decomposition of M^* into right-angled compact generalized polytopes. The truncation produces some new facets that are not gedesically flat, each of which is combinatorially a $(n-1)$-cube. We now define C^* as the cubulation dual to this decomposition of M^*. The term "dual" should be interpreted here in a boundary-respecting sense: every k-stratum in $\mathrm{int}(M)$ and ∂M^* contributes respectively with a $(n-k)$- and a $(n-k-1)$-cube. The vertices of C^* are hence subdivided into the *interior* ones (those of C, dual to the polytopes of the tessellations) and the *boundary* ones (they lie in ∂M^* and are dual to the new non-geodesic cubic facets). The boundary ∂M^* inherits a cubulation ∂C^*, which is dual to the decomposition into the new cubes. We get $M^* = C^*$.

If M is obtained from P by colouring its facets as described above, every vector $v \in \mathbb{Z}_2^c$ determines a polytope P^v of the tessellation and hence a dual vertex of C, that we still denote as v (the letter v can be interpreted both as indicating a $v$ector in $\mathbb{Z}_2^c$ or a $v$ertex in C).

1.4. **Some examples.** Here are some examples.

1.4.1. *The Euclidean n-cube.* We may start with the square $Q \subset \mathbb{R}^2$ coloured with two colors. We get a flat torus M tessellated into four copies of Q. The dual cube complex C here is isomorphic to the tessellation of M itself. This picture easily extends to n-colourings of n-cubes in $\mathbb{R}^n$.

1.4.2. *The ideal regular octahedron.* We may start with an ideal regular octahedron $O \subset \mathbb{H}^3$, coloured with two colors Blue and Red (there is a unique such colouring up to isometry). We get a hyperbolic manifold M with six cusps, one for each ideal

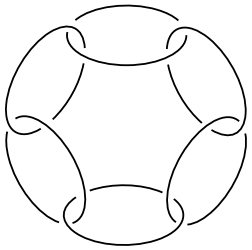

FIGURE 6. The minimally twisted chain link with 6 components.

vertex of O. It is tessellated into four ideal octahedra along the pattern

$$\begin{array}{ccc} O^{01} & \overset{B}{\longleftrightarrow} & O^{11} \\ {\scriptstyle R}\updownarrow & & \updownarrow{\scriptstyle R} \\ O^{00} & \underset{B}{\longleftrightarrow} & O^{10} \end{array}$$

The B and R arrows indicate that the Blue and Red faces should be identified horizontally and vertically, respectively. Each arrow indicates 4 pairs of faces that are coupled. The dual cube complex C has 4 vertices, 16 edges, and 12 squares and is embbeded in M as a spine, that is M collapses onto C. The complement $M \setminus C$ consists of 6 open cusps. The hyperbolic manifold M is in fact the complement of the minimally twisted chain link with 6 components shown in Figure 6, see [20].

At every vertex of O, the cusp section is a Euclidean square, which inherits a Blue / Red colouring. Each Euclidean square gives rise with the same method to a torus cusp section tessellated into four squares.

1.4.3. *The ideal right-angled 24-cell.* We now construct the manifold W that we are going to study, following [20]. We start with the ideal regular right-angled 24-cell $\mathcal{C} \subset \mathbb{H}^4$. This regular polytope has 24 facets, each being a right-angled ideal regular octahedron. It may be coloured in a unique way (up to isometry) with three colors Blue, Red, and Yellow. The 24 octahedral facets are partitioned into 8 Blue, 8 Red, and 8 Yellow facets.

From this colouring we get a cusped hyperbolic 4-manifold W tessellated into eight copies of $\mathcal{C}$ along the pattern

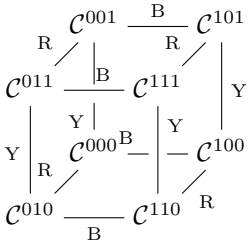

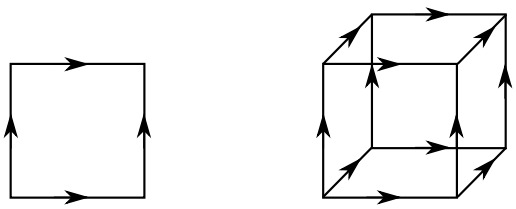

FIGURE 7. Every square (and hence every k-cube) of the cubulation has its opposite edges oriented coherently as shown here.

As above, the edges marked with B, R, Y indicate the identifications of the Blue, Red, and Yellow facets. Every edge indicates 8 pairs of facets that are coupled.

At every ideal vertex of $\mathcal{C}$ we have a Euclidean cube coloured with three colours, that gives rise to a 3-torus cusp section. The manifold W has 24 such cusps, one for each ideal vertex of $\mathcal{C}$.

The manifold W is stratified into 8 ideal 24-cells, 96 ideal octahedra, 192 ideal triangles, and 96 edges. We get $\chi(M) = 8$. This is coherent with the fact that $\chi(\mathcal{C}) = 1$ and W decomposes into 8 copies of $\mathcal{C}$.

2. Diagonal maps

2.1. **Definition.** Let C be a cube complex. We always suppose for simplicity of notation that the link of every vertex v of C is a simplicial complex as this is certainly the case in our examples. A *coherent orientation* on the edges of C is an orientation on the edges, such that on every square the opposite edges are oriented in the same way, as in Figure 7-(left).

If C has a coherent orientation on the edges, following Bestvina – Brady [4] we may construct a piecewise-linear map $f\colon C \to S^1 = \mathbb{R}/\mathbb{Z}$ as follows. The *diagonal map* on the k-cube is the piecewise-linear map

$$[0,1]^k \longrightarrow S^1 = \mathbb{R}/\mathbb{Z}, \qquad x \longmapsto x_1 + \cdots + x_k.$$

The coherent orientation on C allows us to identify unambiguously every cube of the cubulation with the standard k-cube, in such a way that all the diagonal maps match to a global piecewise-linear map $f\colon C \to S^1$. A map f obtained in this way (after fixing a coherent orientation on edges) is also called a *diagonal map* on C.

2.2. **The ascending and descending links.** Let C be a cube complex. Equip C with a coherent orientation on its edges, and $f\colon C \to S^1$ be the diagonal map.

Let v be a vertex of C. Let $\mathrm{link}(v)$ be the link of v in C. By construction $\mathrm{link}(v)$ is an abstract simplicial complex. Every vertex of $\mathrm{link}(v)$ indicates an edge incident to v, and we assign to it the *status* I (In) or O (Out) according to whether the edge points towards v or away from v.

Following [4], we define the *ascending link* $\mathrm{link}_\uparrow(v)$ (respectively, *descending link* $\mathrm{link}_\downarrow(v)$) to be the subcomplex of $\mathrm{link}(v)$ generated by all the vertices with status O (respectively, I).

The following theorem is proved in [4].

Theorem 15. *If the descending and ascending link at every vertex v of C are connected, the kernel of $\pi_1(C) \to \pi_1(S^1)$ is finitely generated.*

2.3. **Geometric manifolds.** Let M be a finite-volume spherical, flat, or hyperbolic n-manifold that is tessellated into finitely-many right-angled polytopes. For instance, the manifold M might be constructed starting from a single polytope P via the colouring construction described in Section 1 (all the examples that we study in this paper will be of this type).

Let $C \subset M$ be the cube complex dual to the tessellation of M. We indicate with C both the cube complex and its support. If M is compact we have $M = C$. If not, we enlarge C to C^* as described in Section 1.3 and get $M^* = C^*$.

Let now C be equipped with a coherent orientation on the edges. We get a diagonal map $f\colon C \to S^1$. If M is compact, we have $M = C$, we get $f\colon M \to S^1$ and we are happy. If M is cusped, there is a non-ambiguous way to extend the coherent orientation from C to C^*, by assuming that all the edges that connect an interior vertex to a boundary vertex are oriented towards the boundary. The extended coherent orientation on C^* produces a diagonal map $f\colon C^* \to S^1$.

In any case (M compact or M cusped) a coherent orientation on the edges of C produces a *diagonal map* $f\colon M \to S^1$. In the cusped case this map is the restriction of a map $f\colon M^* \to S^1$.

2.4. **Trivial and Hopf links.** We work in the piecewise-linear (PL) category, see [27] for an introduction. The cube complexes C and C^* have a natural PL structure. For every $0 \leq i \leq n$, we let the *Hopf link of index i* be the PL submanifold of S^{n-1}

$$\big(\partial D^i \times 0\big) \sqcup \big(0 \times \partial D^{n-i}\big) \subset \partial(D^i \times D^{n-i}) = \partial D^n = S^{n-1}.$$

In all cases we think of the Hopf link as a partition $A \sqcup B$ into two (possibly empty, possibly disconnected) disjoint submanifolds A and B of S^{n-1}. In the extremal cases $i = 0$ and $i = n$, the Hopf link is $\emptyset \sqcup S^{n-1}$ and $S^{n-1} \sqcup \emptyset$. When $n = 4$ and $i = 2$ we get the usual Hopf link in S^3.

Let as above M be a spherical, flat, or hyperbolic finite-volume manifold tessellated into right-angled polytopes, with dual cube complex C. Let v be a vertex of C, dual to some polytope P of the tessellation. If P is compact we have $\mathrm{link}(v) = S^{n-1}$, while if P has some ideal vertices we have $\mathrm{link}(v) \subset S^{n-1}$ and the complement $S^{n-1} \setminus \mathrm{link}(v)$ consists of the open interior of an $(n-1)$-octahedron O (the dual of a $(n-1)$-cube) around each ideal vertex of P.

In the cusped case we might sometimes want to consider the extended cube complex C^*. The difference between $\mathrm{link}^C(v)$ and $\mathrm{link}^{C^*}(v)$ for a vertex v of C is

that in the latter the complementary open $(n-1)$-octahedra are each filled with 2^{n-1} distinct $(n-1)$-simplexes with a new central vertex, so that $\mathrm{link}^{C^*}(v) = S^{n-1}$. When we write $\mathrm{link}(v)$ we always mean $\mathrm{link}^{C}(v)$.

Let now C be equipped with a coherent orientation of the edges. Let v be a vertex of C, dual to a polytope P of the tessellation. The ascending and descending links at v are subsets of $\mathrm{link}(v) \subset S^{n-1}$.

Definition 16. The subcomplex $\mathrm{link}_\downarrow(v) \sqcup \mathrm{link}_\uparrow(v) \subset \mathrm{link}(v) \subset S^{n-1}$ is

- *trivial* if it collapses to a pair of points;
- *of Hopf type* with index i, if it collapses to a Hopf link in S^{n-1} of index i.

If P is not compact, in both cases we also require the following: for every ideal vertex of P the corresponding $(n-1)$-octahedron $O \subset S^{n-1}$ with $O \cap \mathrm{link}(v) = \partial O$ is such that $O \cap (\mathrm{link}_\downarrow(v) \sqcup \mathrm{link}_\uparrow(v))$ is trivial, that is it collapses to a pair of points.

We say that v is *trivial* or *of Hopf type* if the pair $\mathrm{link}_\downarrow(v) \sqcup \mathrm{link}_\uparrow(v)$ is. Of course this definition depends not only on v but also on the chosen coherent orientation on the edges of C. We now aim at proving the following theorem.

Theorem 17. *If $n \leq 7$ and every vertex v of C is either trivial or of Hopf type, the diagonal map $f\colon M \to S^1$ can be smoothened to a circle-valued Morse function with one critical point of index i at each vertex of C of Hopf type with index i.*

As we will see, the dimension restriction $n \leq 7$ is needed only to ensure that one can transform a PL handle into a smooth one. The rest of the section is devoted to the proof of Theorem 17.

2.5. **Handles.** Let as above M be a spherical, flat, or hyperbolic finite-volume manifold tessellated into right-angled polytopes, with dual cube complex C. Let C be equipped with a coherent orientation on its edges. We get a diagonal map $f\colon M \to S^1$. When M is cusped this is the restriction of $f\colon M^* \to S^1$.

The diagonal map $f\colon M \to S^1$ lifts to a map $\tilde{f}\colon \widetilde{M} \to \mathbb{R}$ where $\widetilde{M} \to M$ is the covering determined by the kernel of $f_*\colon \pi_1(M) \to \pi_1(S^1) = \mathbb{Z}$. Similarly we get a map $\tilde{f}\colon \widetilde{M}^* \to \mathbb{R}$ in the cusped case. The cubulations C and C^* lift to cubulations $\widetilde{C}$ and $\widetilde{C}^*$ for $\widetilde{M}$ and $\widetilde{M}^*$.

We study the PL map $\tilde{f}\colon \widetilde{M} \to \mathbb{R}$. As in [4], for any non-empty closed subset $J \subset \mathbb{R}$ we are interested in its counterimage $\widetilde{M}_J = \tilde{f}^{-1}(J)$. We write $\widetilde{M}_t = \widetilde{M}_{\{t\}}$. The following is analogous to [4, Lemma 2.3].

Theorem 18. *If $J = [a, b]$ is an interval with endpoints $a, b \notin \mathbb{Z}$, the counterimage $\widetilde{M}_J$ is a PL manifold with boundary*

$$\partial \widetilde{M}_J = \widetilde{M}_a \sqcup \widetilde{M}_b.$$

If $[a, b] \cap \mathbb{Z} = \emptyset$, the manifold $\widetilde{M}_J$ is PL homeomorphic to the product

$$\widetilde{M}_J = \widetilde{M}_a \times [a, b].$$

Proof. It suffices to prove the second assertion, since it easily implies the first. If $[a,b]\cap\mathbb{Z}=\emptyset$, the counterimage $\widetilde{M}_J$ is a union of prisms and is hence PL homeomorphic to $\widetilde{M}_a\times[a,b]$. Since its interior $\widetilde{M}_a\times(a,b)$ is an open subset of $\widetilde{M}$, it is a PL n-manifold, and hence $\widetilde{M}_a$ is a PL $(n-1)$-manifold, see [27, Exercise 2.24(3)]. □

When M has cusps, the map $f\colon \widetilde{M}\to\mathbb{R}$ is the restriction of $f\colon \widetilde{M}^*\to\mathbb{R}$ and a similar assertion holds for $\widetilde{M}^*$, with an analogous proof. We write again $\widetilde{M}^*_J=\tilde{f}^{-1}(J)$ and $\widetilde{M}^*_t=\widetilde{M}^*_{\{t\}}$.

Theorem 19. *If $J=[a,b]$ is an interval with endpoints $a,b\notin\mathbb{Z}$, the counterimage $\widetilde{M}^*_J$ is a PL manifold with boundary*

$$\partial\widetilde{M}^*_J=\widetilde{M}^*_a\cup\widetilde{M}^*_b\cup(\widetilde{M}^*_J\cap\partial\widetilde{M}^*).$$

If $[a,b]\cap\mathbb{Z}=\emptyset$, the manifold $\widetilde{M}^*_J$ is PL homeomorphic to the product

$$\widetilde{M}^*_J=\widetilde{M}^*_a\times[a,b].$$

We are now left to consider the case where the interior of $[a,b]$ contains some integer. This is where the ascending and descending links play a fundamental role.

Theorem 20. *Let $t\in\mathbb{Z}$ be fixed. Suppose that every vertex v of C with $f(v)=t$ is either trivial or of Hopf type with some index i.*

Then for every $0<\varepsilon<1$ and $a<t-\varepsilon, a\notin\mathbb{Z}$ the manifold $\widetilde{M}_{[a,t+\varepsilon]}$ is PL homeomorphic to $\widetilde{M}_{[a,t-\varepsilon]}$ with one i-handle attached to $\widetilde{M}_{t-\varepsilon}$ for each vertex v with $f(v)=t$ of Hopf type with index i.

When M has cusps, the same assertion holds also for $\widetilde{M}^*$.

Proof. We consider first the case where M is compact. In this case, as shown in [4, Lemma 2.5], the submanifold $\widetilde{M}_{[a,t+\varepsilon]}$ collapses onto $\widetilde{M}_{[a,t-\varepsilon]}\cup\big(\cup_v C_v\big)$ where C_v is a cone over $\mathrm{link}_\downarrow(v)$, considered inside $\widetilde{M}_{t-\varepsilon}$, and v varies among all the vertices with $f(v)=t$.

By hypothesis v is either (i) trivial or (ii) of Hopf type, and this implies that C_v collapses either (i) to a point in $\widetilde{M}_{t-\varepsilon}$ or (ii) to a i-disc D^i with $\partial D^i\subset\widetilde{M}_{t-\varepsilon}$. Therefore the manifold $\widetilde{M}_{[a,t+\varepsilon]}$ collapses to $\widetilde{M}_{[a,t-\varepsilon]}\cup(\cup D^i)$, and is hence PL homeomorphic to $\widetilde{M}_{[a,t-\varepsilon]}$ with a i-handle attached for each vertex v of Hopf type with index i, as required.

When M has cusps, we prove the theorem for $\widetilde{M}^*$, and the same assertion for $\widetilde{M}$ then follows trivially. By the (already proved) compact case, the condition on the $(n-1)$-octahedra in Definition 16 implies that $\partial\widetilde{M}^*\cap\widetilde{M}^*_{[t-\varepsilon,t+\varepsilon]}$ is a product, so the boundary behaves as required.

For each interior vertex v of C^* with $f(v)=t$, the hypothesis on the $(n-1)$-octahedra in Definition 16 implies that each $\mathrm{link}^{C^*}_\downarrow(v)$ and $\mathrm{link}^{C^*}_\uparrow(v)$ collapses unto $\mathrm{link}^{C}_\downarrow(v)$ and $\mathrm{link}^{C}_\uparrow(v)$. So all the proof for M compact applies also in this case. □

We can finally prove Theorem 17.

Proof of Theorem 17. By Theorems 18 and 20 the function f determines a circular handle decomposition for M, where we start with a regular fiber, add a i-handle whenever we cross a vertex v of Hopf type with index i, and then come back to the regular fiber. Since $n \leq 7$, this circle-valued handle decomposition can be smoothened [12, 25]. The smooth circle-valued handle decomposition can then be transformed into a circle-valued Morse function. □

As we already mentioned, the dimension restriction $n \leq 7$ is there only to ensure that PL handles can be smoothened, and it is not needed if we are able to do this in some way.

2.6. **Examples.** We describe a few simple examples. Some more elaborate ones will be constructed in the next section.

2.6.1. *The n-torus.* Pick the Euclidean n-cube P and identify the opposite facets via translations to get the flat n-torus M. The dual cube complex C is isomorphic to the tessellation of M itself. There is only one coherent orientation on the edges of C up to combinatorial isomorphisms of C.

There is a unique vertex v in C, and the simplicial complex $\mathrm{link}(v)$ is isomorphic to the boundary of a n-octahedron. The descending and ascending links are two opposite $(n-1)$-simplexes in $\mathrm{link}(v)$. Therefore v is trivial and Theorem 17 applies. The map f can be smoothened (in fact, it is already so) to a circle-valued Morse function without critical points, that is a fibration.

2.6.2. *The genus-g hyperbolic surface.* Consider a genus-g surface S_g with $g \geq 2$. Pick two transverse multicurves $\alpha, \beta \subset S_g$ that decompose S_g into hexagons. Orient transversely α and β. Assign to each hexagon the structure of a right-angled regular hyperbolic hexagon. We get a tessellation of S_g into right-angled hexagons.

The transverse orientations on α and β furnish a coherent orientation on the edges of the dual cubulation C. For every vertex v of C the simplicial complex $\mathrm{link}(v) = S^1$ is the boundary of a hexagon. Depending on the chosen coherent orientation, the pair $\mathrm{link}_\downarrow(v) \sqcup \mathrm{link}_\uparrow(v)$ may collapse to one of the following:

$$S^1 \sqcup \emptyset,\ \{1\text{ point}\} \sqcup \{1\text{ point}\},\ \{2\text{ points}\} \sqcup \{2\text{ points}\},\ \{3\text{ points}\} \sqcup \{3\text{ points}\},\ \emptyset \sqcup S^1.$$

The pair is trivial in the second case, and of Hopf type (with index $0, 1, 2$) in the first, third, and last case. If the fourth case never occurs for any v, then Theorem 17 applies. If it occurs at some vertex v, the theorem cannot be applied. We note that in this case the function f looks near v like a monkey saddle and hence it cannot be smoothened to a Morse function with a single critical point.

2.6.3. *More on flat manifolds tessellated by n-cubes.* Let a flat n-manifold M be tessellated into some cubes. For every vertex v of the dual cube complex C, the simplicial complex $\mathrm{link}(v)$ is the boundary of a n-octahedron. It is an easy exercise (proved by induction on n) that, no matter how the edges incident to v are oriented,

the descending and ascending links in link(v) will always be either trivial or of Hopf type with some index i. (This is not the case when link(v) is more complicated, for instance if it is the boundary of a hexagon as in the previous example.) This implies that Theorem 17 applies to any chosen coherent orientation on the edges.

3. States

We now combine the techniques exposed in Sections 1 and 2. The bridge between the two sections is the notion of *state* introduced in [14].

3.1. **States.** Let $P \subset \mathbb{X}^n$ be a finite right-angled polytope in some space $\mathbb{X}^n = \mathbb{H}^n, \mathbb{R}^n$ or $\mathbb{S}^n$. Following [14], a *state* is a partition of the facets of P into two subsets, that we call I (in) and O (out). Every facet inherits a *status* I or O.

We fix a colouring for P, with colours $\{1, \dots, c\}$. The colouring induces a free action of $\mathbb{Z}_2^c$ on the set of all states of P, as follows. The element e_i acts by toggling the IO status of every facet coloured by i, and leaving the status of the other facets unaffected. The action is free, so each orbit consists of 2^c distinct states.

3.2. **A state defines a coherent orientation.** Fix a colouring on P. As described in Section 1, the colouring produces a subgroup $\Gamma' \lhd \Gamma < \mathrm{Isom}(\mathbb{X}^n)$ and a manifold $M = \mathbb{X}^n/_{\Gamma'}$ tessellated into 2^c copies of P, denoted by P^v as $v \in \mathbb{Z}_2^c$ varies. The vertices of the dual cube complex C are identified with $\mathbb{Z}_2^c$.

Fix a state s on P. This induces an orientation on all the edges of C, as follows. By construction an edge of C connects v to $v+e_i$ for some i and some v with $v_i = 0$ (here v_i is the i-th coordinate of v) and there is one edge connecting v to $v + e_i$ for every facet F of P coloured with i (many edges may have the same endpoints, since many facets of P may have the same colour). We orient this edge towards $v + e_i$ if the status of F is O, and towards v if the status of F is I. The resulting orientation for the edges of C is coherent, since the parallel edges connecting v to $v + e_i$ and w to $w + e_i$ are oriented in the same manner.

The fixed state s on P induces a coherent orientation on all the edges of C, and this in turn defines an *induced state* at every P^v, obtained by assigning the status I or O at every vertex of link(v) according to whether the corresponding edge points towards v or not. It is easy to see that the induced state of P^v is precisely $v(s)$, the image of the initial state s under the action of v. So in particular the induced state of P^0 is s itself. We can say that the polyhedron P^v inherits the same colours of P, but not the same state s of P. It gets instead the state $v(s)$.

Summing up: if we assign a colouring and a state to P, we get a manifold M and a coherent orientation on the edges of the dual cubulation C. This in turn produces a diagonal map $f\colon M \to S^1$ as discussed in Section 2. Shortly:

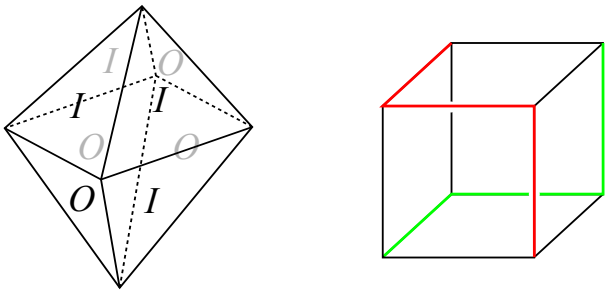

FIGURE 8. A state for the right-angled ideal regular octahedron (left) and the corresponding descending (red) and ascending (green) link (right).

colouring + state on $P \Longrightarrow$ manifold M + coherent orientation on C
$\Longrightarrow$ diagonal map $f\colon M \to S^1$.

If the ascending and descending links are all of trivial or Hopf type, Theorem 17 applies and the diagonal map $f\colon M \to S^1$ can be smoothened to a circle-valued Morse function. The ascending and descending link at v are simply the simplicial complexes generated by the vertices with status O and I in $v(s)$.

3.3. **Examples.** We now assign colourings and states to some right-angled polytopes P to produce manifolds M with interesting diagonal functions $f\colon M \to S^1$.

3.3.1. *The n-cube.* Let P be the n-cube, coloured with n colours. Opposite faces have the same colour. The manifold M is a flat n-torus.

Fix an arbitrary state s on P. The polytope P^v inherits the state $v(s)$. As shown in Section 2.6.3, every vertex will be either trivial or of Hopf type, so Theorem 17 applies for any initial choice of s.

If in the state s there is a pair of opposite facets with opposite status, it is easy to deduce that this condition holds at $v(s)$ for every v, and all the vertices are trivial. Hence $f\colon M \to S^1$ can be smoothened to be a fibration.

On the other hand, if every pair of opposite facets share the same status in s, then every v is of Hopf type with some index i that varies with v. When smoothened, we get a Morse function on the n-torus with $\binom{n}{i}$ critical points of index i. We will prove in Proposition 24 that the map f is homotopic to a constant in this case.

3.3.2. *The ideal regular octahedron.* Let $O \subset \mathbb{H}^3$ be the ideal regular octahedron coloured with two colours. We get the hyperbolic manifold M with 6 cusps already considered in Section 1.4.2. As shown in [14], we can give O the state s depicted in Figure 8-(left). One checks easily that $v(s)$ is equivalent to s via an isometry of O, for all $v \in \mathbb{Z}_2^2$.

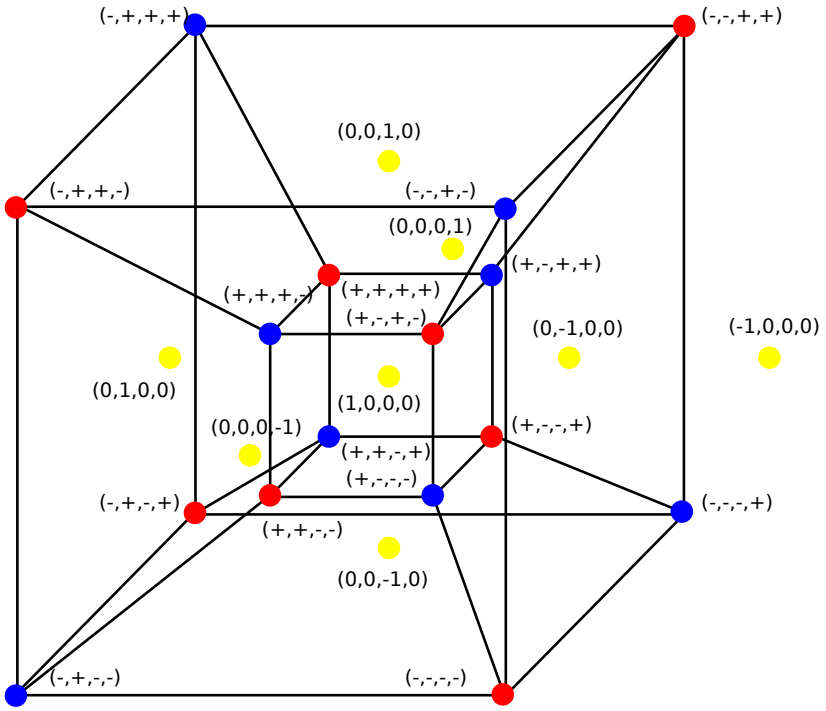

FIGURE 9. The vertices of the dual 24-cell $\mathcal{C}^*$ coloured in Blue, Red, and Yellow.

For every $v \in C$, the simplicial complex $\mathrm{link}(v) \subset S^2$ is the 1-skeleton of a cube. The descending and ascending links form the trivial pair shown in Figure 8-(right). Therefore $f\colon M \to S^1$ can be smoothened to a smooth fibration.

3.3.3. *The ideal 24-cell.* Let $\mathcal{C}$ be the ideal 24-cell coloured with three colours. We get the manifold W with 24 cusps already described in Section 1.4.3 and studied in [20, 23].

The 24-cell is self-dual. Therefore we may represent the facets of $\mathcal{C}$ as the vertices of the dual 24-cell $\mathcal{C}^*$. The vertices of the dual 24-cell $\mathcal{C}^*$ are shown in Figure 9. We write $(\pm,\pm,\pm,\pm)$ for $\left(\pm\frac{1}{2},\pm\frac{1}{2},\pm\frac{1}{2},\pm\frac{1}{2}\right)$. The figure shows the Blue, Red, and Yellow colouring of the facets of $\mathcal{C}$. For simplicity, the figure displays only some of the edges of $\mathcal{C}^*$, that altogether form the 1-skeleton of a 4-cube: more edges should be added that connect each yellow vertex with 8 nearby blue or red vertices. We can interpret the red and blue vertices $(\pm,\pm,\pm,\pm)$ as the vertices of a hypercube, and the yellow vertices $\pm e_i$ as the (centers of) the facets of the hypercube. This convenient kind of picture is taken from [14].

As a state s for $\mathcal{C}$, we choose the one shown in Figure 10-(right), with black and white vertices representing the status I and O respectively. Figure 10-(left) shows

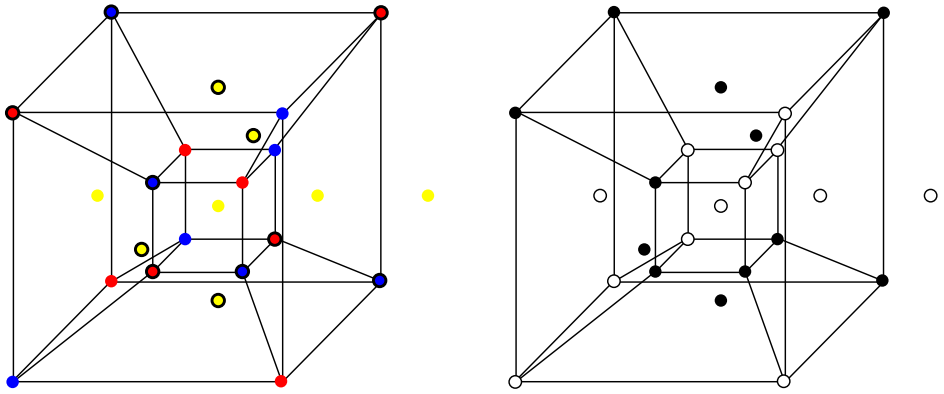

FIGURE 10. The state s of the 24-cell. The black and white vertices of $\mathcal{C}^*$ represent the status I and O respectively (right). In the left figure we show both the colouring and the state.

both the colouring and the state of $\mathcal{C}$. This state is taken from [14], where a family of convenient states is described that includes also this one.

The state s is quite remarkable and contains more symmetries than the ones we can infer by looking at Figure 10. For instance, we now prove that the orbit $v(s)$ as $v \in \mathbb{Z}_2^3$ varies consists of 8 isometric states. The proof also shows that s can be nicely described using quaternions.

Proposition 21. *All the states $v(s)$ are isometric to s, for all $v \in \mathbb{Z}_2^3$.*

Proof. This surprising fact is not obvious from the picture and can be proved using quaternions. Some of the terms and arguments that we expose in this proof will also be used at some point in the subsequent pages.

If we interpret (a, b, c, d) as the quaternion $a + bi + cj + dk$, we note that the vertices of $\mathcal{C}^*$ form the binary tetrahedral group T_{24}^*. The yellow vertices form an index-3 normal subgroup $Q_8 \triangleleft T_{24}^*$ and the red and yellow vertices are the two other lateral classes of Q_8.

Let L_q and R_q denote the left- and right-multiplication by the quaternion q. The isometry $L_i \colon \mathcal{C}^* \to \mathcal{C}^*$ preserves each lateral class of 8 vertices (an *octet*), and subdivides it into two orbits of 4 vertices (a *quartet*). In Figure 10 we have given the status I to one quartet and O to the other, inside each octet. The choice of which quartet is I and which is O inside each octet is arbitrary, but it does not affect much the result: the orbit $\{v(s), v \in \mathbb{Z}_2^3\}$ consists precisely in the 8 states that can be obtained in this way.

Every isometry of $\mathcal{C}^*$ preserves the partition into octets, but not all the isometries preserve the partition into quartets. Since they (anti-)commute with L_i, the isometries L_j, L_k, R_q do preserve the partition into quartets for all $q \in \mathcal{C}^*$. By looking at Figures 9 and 10 we check easily that:

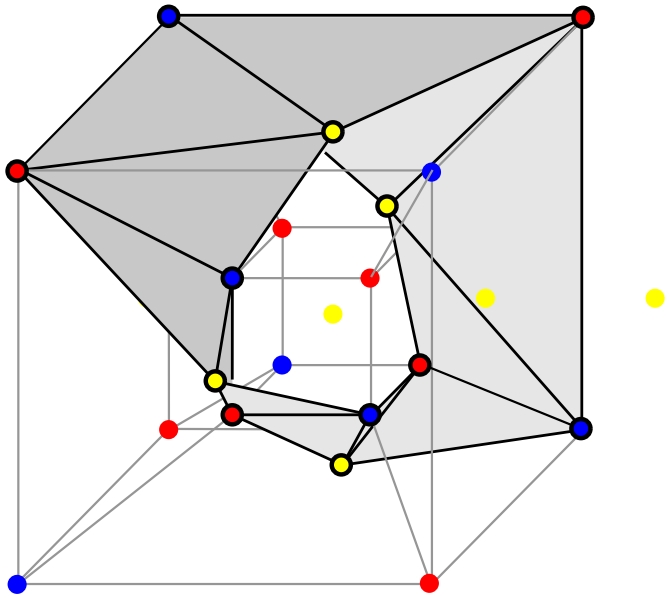

FIGURE 11. The descending link is a band decomposed into 12 triangles. The ascending link is isomorphic to it, and altogether they form two bands that collapse onto a Hopf link in S^3.

- L_j, L_k interchange the pairs of quartets in each octet,
- R_i, R_j, R_k interchange the pairs of quartets in the two octets BR, RY, and YB respectively, and leaves the third pair unaffected.

By composing these we realize any permutation of the quartets while keeping the octets fixed. We deduce that $v(s)$ is isometric to s for any $v \in \mathbb{Z}_2^c$. □

The state s of $\mathcal{C}$ induces a diagonal map $f\colon W \to S^1$. We can prove Theorem 2.

Theorem 22. *Every vertex v is of Hopf type with index 2. Therefore f can be smoothened to a circle-valued Morse function $f\colon W \to S^1$ with 8 critical points of index 2.*

Proof. For every vertex $v \in \mathbb{Z}_2^3$ of the dual cube complex C, the simplicial complex $\mathrm{link}(v) \subset S^3$ is the 2-skeleton of the dual 24-cell $\mathcal{C}^*$. It is easy to deduce from Figure 10 that the descending and ascending links are of Hopf type with index 2. Indeed they form two bands that collapse onto a Hopf link in S^3, see Figure 11. We apply Theorem 17. □

Remark 23. Among the many remarkable properties of the ideal right-angled 24-cell $\mathcal{C}$ there is the fact that $\chi(\mathcal{C}) = 1$. A hyperbolic 4-manifold M that decomposes into k copies of $\mathcal{C}$ has $\chi(M) = k$, and therefore M is allowed to have a circle-valued

Morse function $f\colon M \to S^1$ with one index-2 critical point inside each copy of $\mathcal{C}$. We have just constructed a function $f\colon W \to S^1$ of this type.

This is not the case for instance for the right-angled compact 120-cell P, that has $\chi(P) = \frac{17}{2}$. Since $\frac{17}{2} > 1$, Theorem 17 cannot be applied on any manifold M that decomposes into some copies of P, because it would give a forbidden too small number of critical points.

4. The regular and singular fibers

In the previous section we have constructed some interesting circle-valued Morse functions $f\colon M \to S^1$. We now describe a combinatorial method for identifying the regular M^{reg} and singular fibers M^{sing} of the function. It is in general easier to work with the lifted function $\tilde{f}\colon \widetilde{M} \to \mathbb{R}$.

4.1. **The homomorphism f_*.** As in Section 3, let $P \subset \mathbb{X}^n$ be a finite right-angled polytope in some space $\mathbb{X}^n = \mathbb{H}^n, \mathbb{R}^n$ or $\mathbb{S}^n$, equipped with a colouring with c colours and a state s. From this data we get a manifold M tessellated into polytopes P^v with $v \in \mathbb{Z}_2^c$ and a diagonal map $f\colon M \to S^1$.

At the level of fundamental groups we have a dichotomy, already encountered in a specific case in Section 3.3.1.

Proposition 24. *Precisely one of the following holds:*

1. *If facets of P with the same colour always have the same status, the map f is homotopic to a constant.*
2. *If there are two facets in P with the same colour and opposite status, the homomorphism $f_*\colon \pi_1(M) \to \pi_1(S^1) = \mathbb{Z}$ is non-trivial with image $2\mathbb{Z}$.*

Proof. If (1) holds for the state s, it holds for every state $v(s)$, for all $v \in \mathbb{Z}_2^c$. We may lift the map $f\colon M \to S^1$ to a map $\tilde{f}\colon M \to \mathbb{R}$ as follows. For each vertex $v \in \mathbb{Z}_2^c$ of the dual cube complex C we define $\tilde{f}(v) \in \mathbb{Z}$ as the maximum number of facets of P^v with distinct colours with status O. The map $\tilde{f}$ extends diagonally on every cube of C, and then of C^* in the cusped case. Therefore f is homotopic to a constant.

If (2) holds, the two facets coloured with i with opposite status determine two edges of C connecting 0 and e_i oriented in opposite directions. They form a loop whose image runs twice around S^1. Hence $2 \in \mathrm{Im}(f_*)$.

Finally, we note that $1 \notin \mathrm{Im}(f_*)$ because the 1-skeleton of C is naturally bipartited: a vertex v is *even* or *odd* according to the sum $v_1 + \ldots + v_c$ and every edge connects two vertices of opposite parity. □

We will henceforth suppose that (2) holds. It then makes sense to consider the covering $\widetilde{M} \to M$ associated to $\ker f_*$.

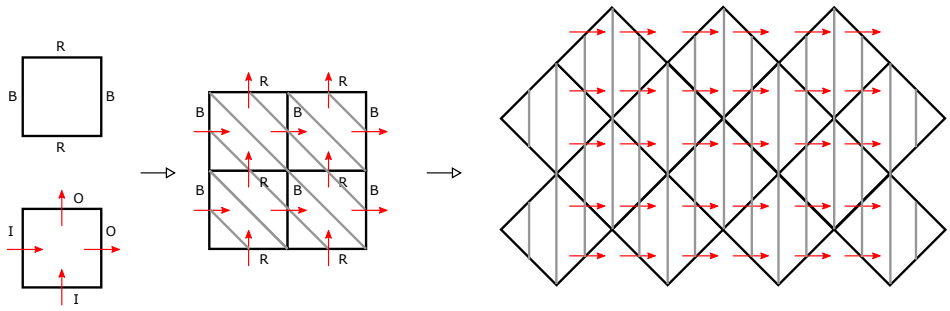

FIGURE 12. The manifold $\widetilde{M}$ when P is a square with the colours and state indicated on the left. The central figure shows the torus M tessellated into four squares (the opposite external vertical and horizontal edges should be identified), and the fibration $f\colon M \to S^1$ is suggested by the red arrows, with some fibers drawn in grey. The manifold $\widetilde{M}$ is the infinite annulus shown on the right (the zigzagged top and bottom edges should be identified), and the fibration $\tilde{f}\colon \widetilde{M} \to \mathbb{R}$ is also suggested by the red arrows, with some fibers drawn in grey (so $\tilde{f}$ is the projection on the horizontal axis).

The covering manifold $\widetilde{M}$ and its tessellation. The tessellation of M into polytopes P^v lifts to a tessellation for $\widetilde{M}$ into polytopes P^v_t, parametrized by $v \in \mathbb{Z}_2^c$ and $t \in \mathbb{Z}$, with the requirement that $v_1 + \cdots + v_c + t$ is even.

The facet F of P^v_t is identified with the identity map to the corresponding facet of $P^{v+e_i}_{t\pm1}$, where i is the colour of F and the sign $+1$ or -1 depends on whether the status of F in P^v_t is O or I.

The covering $\widetilde{M} \to M$ is the forgetful map $P^v_t \to P^v$. The monodromy of the covering $\widetilde{M} \to M$ is the map $\tau\colon \widetilde{M} \to \widetilde{M}$ that sends P^v_t to P^v_{t+2} identically.

The cubulation C (and C^* if there are cusps) in M lifts to a cubulation $\widetilde{C}$ (and $\widetilde{C}^*$ if there are cusps) in $\widetilde{M}$. The vertices of $\widetilde{C}$ are parametrized by the pairs (v,t) with $v \in \mathbb{Z}_2^c, t \in \mathbb{Z}$ and $v_1 + \cdots + v_c + t$ even. The vertex (v,t) is dual to P^v_t.

The lifted map $\tilde{f}\colon \widetilde{M} \to \mathbb{R}$ sends the vertex (v,t) of $\widetilde{C}$ to t and is extended diagonally on $\widetilde{C}$ (and on $\widetilde{C}^*$ if there are cusps). See an instructing example with the square in Figure 12.

Remark 25. In all the examples we are interested in, the fiber $f^{-1}(t)$ of $f\colon M \to S^1 = \mathbb{R}/\mathbb{Z}$ has exactly two components for all $t \in S^1$. When $t = 0$, the vertices of $\mathbb{Z}_2^c$ with different parity lie on distinct components of $f^{-1}(0)$. See for instance in Figure 13 the square case, where each fiber consists of two circles. This is connected to the fact that the image of f_* is $2\mathbb{Z}$ and not $\mathbb{Z}$, and it is only a slightly confusing but not important issue since of course the fibration can be unwrapped to get connected

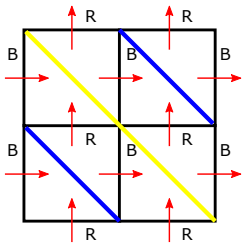

FIGURE 13. The fiber of $f\colon M \to S^1$ above a point has at least two components: here M is the torus considered in Figure 12 and the fiber above any point consists of two circles (yellow and blue).

fibers. Anyway, the fiber of $\tilde{f}\colon \widetilde{M} \to \mathbb{R}$ is connected for all t, and also for this reason it is often preferable to work with $\widetilde{M}$ than M.

The *level* of a vertex (v,t) of $\widetilde{C}$ is the number t, that is its image along $\tilde{f}$. More generally, the *level* of a k-cube in $\widetilde{C}$ is the average of the levels of its vertices, that is the image of its center along $\tilde{f}$. This number lies in $\mathbb{Z}$ or in $\mathbb{Z}+\frac{1}{2}$ according to the parity of k. The level of every k-stratum of the tessellation into polytopes $\{P_t^v\}$ is by definition the level of its dual $(n-k)$-cube.

Every facet F of the tessellation is adjacent to P_t^v and $P_{t+1}^{v+e_i}$ and has level $t+\frac{1}{2}$. Every codimension-two face is adjacent to four polytopes

$$P_{t-1}^{v}, P_t^{v+e_i}, P_t^{v+e_j}, P_{t+1}^{v+e_i+e_j}$$

and has level t.

4.2. **The regular and singular fibers.** Two types of fibers in the map $f\colon \widetilde{M} \to \mathbb{R}$ are of interest for us. The first one is $M^{\mathrm{sing}} = \tilde{f}^{-1}(t)$ for some $t \in \mathbb{Z}$. We call it a *singular fiber* because it is often singular. The second one is $M^{\mathrm{reg}} = \tilde{f}^{-1}(t+\frac{1}{2})$, and we call it a *regular fiber*. The regular fiber is guaranteed to be a manifold by Theorem 18, and in fact the fibers $\tilde{f}^{-1}(t+\varepsilon)$ with $\varepsilon \in (0,1)$ are all isotopic. We now characterize both the singular and the regular fibers up to isotopy. We work in the PL category.

We first note that the singular and regular fibers depend only on the parity of $t \in \mathbb{Z}$, because the deck transformation τ sends $\tilde{f}^{-1}(u)$ to $\tilde{f}^{-1}(u+2)$. In all the cases we are interested in, we also have $\tilde{f}^{-1}(u) = \tilde{f}^{-1}(u+1)$ thanks to some additional symmetries. So we often drop t from the notation and write the two fibers as M^{sing} and M^{reg}.

Our intuition is guided by Figure 14. In the figure, the singular and regular fibers are isotopic to some (blue and yellow) subsets that are combinatorially easy to describe. The blue subset is a union of cones, one in each P_t^v. The yellow subset is simply the union of all the facets with level $t+\frac{1}{2}$.

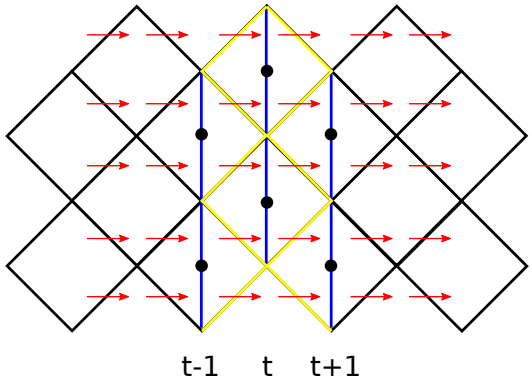

FIGURE 14. In many cases the singular and the regular fibers can be isotoped to the blue and yellow subsets shown here. The blue subset is made of cones over some codimension-2 faces. The yellow subset consists of all the facets with the same level.

We define these blue cones. Consider a polytope P_t^v. Note that the facets of P_t^v with status O and I are precisely those with level $t+\frac{1}{2}$ and $t-\frac{1}{2}$. A codimension-2 face of P_t^v has level $t-1, t, t+1$ if it separates two facets of P_t^v with status II, IO, or OO respectively.

We define $C_t^v \subset P_t^v$ as the cone from an interior point of P_t^v over all the codimension-2 faces of P_t^v that have level t. These are precisely the codimension-2 faces of P_t^v that separate two facets with two opposite status.

We now show that indeed the singular and regular fibers are isotopic to the blue and yellow subsets, at least in the small dimensions we are interested in.

Proposition 26. *Suppose that $n \leq 3$, or $n = 4$ and P has only ideal vertices. The singular M^{sing} and regular M^{reg} fiber in $\widetilde{M}$ are isotopic respectively to the following subsets:*

- *The union of C_t^v as v varies.*
- *The union of all the $(n-1)$-strata of level $t+\frac{1}{2}$.*

Proof. We do not know if the dimensional restrictions in the hypothesis are really necessary, but these allow us to prove everything more comfortably by staring at some tridimensional pictures that will also be used in the next pages.

By hypothesis the dual cubulation $\widetilde{C}$ has dimension ≤ 3. We first consider the case where M is compact. If $\dim M = 3$, we modify the fibers inside each cube of $\widetilde{C}$ as shown in Figure 15 and we are done. If $\dim M = 2$ the picture is simpler.

If there are cusps, we perform the isotopies of Figure 15 on $\widetilde{C}$, and we extend them productwise on each cube of $\widetilde{C}^* \setminus \widetilde{C}$. Therefore the theorem holds also when $\dim M = 4$ and P has only ideal vertices. □

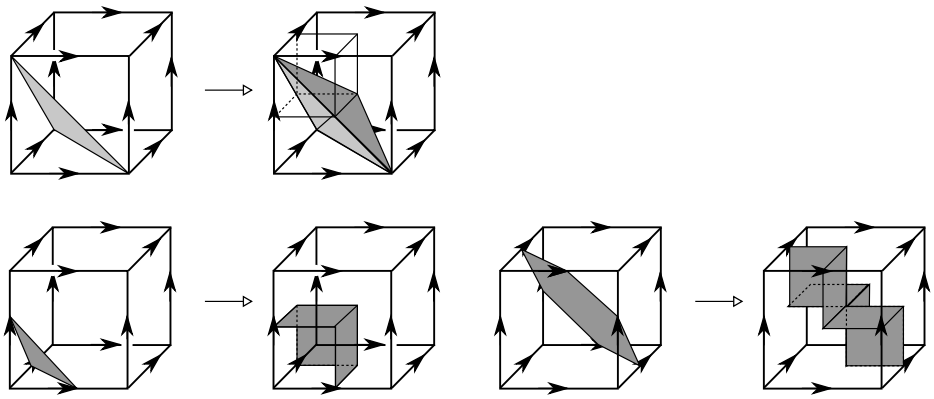

FIGURE 15. How to isotope the singular (top) and regular (bottom) fibers, to transform them into the blue and yellow subsets of Proposition 26.

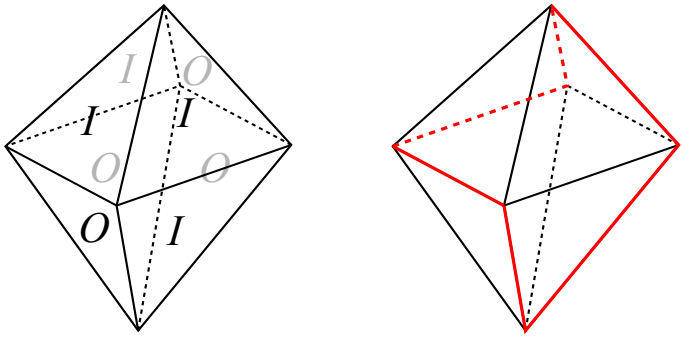

FIGURE 16. The state on the octahedron (left). The closed curve that separates the I and O faces (right).

4.3. **Examples.** We now use Proposition 26 to determine the regular and singular fibers of the examples of Section 3.3.

4.3.1. *The square.* The singular and regular fibers for the square are isotopic to the blue and yellow PL simple closed curves shown in Figure 14.

4.3.2. *The regular ideal octahedron.* Let $O \subset \mathbb{H}^3$ be the ideal regular octahedron coloured with two colours. We equip O with the state described in Section 3.3.2 and reported in Figure 16-(left). We get a hyperbolic manifold M with 6 cusps and a fibration $f\colon M \to S^1$. We can identify the fiber of f.

Proposition 27. *The fiber of the bundle $f\colon M \to S^1$ is a sphere with six punctures, one for each cusp of M.*

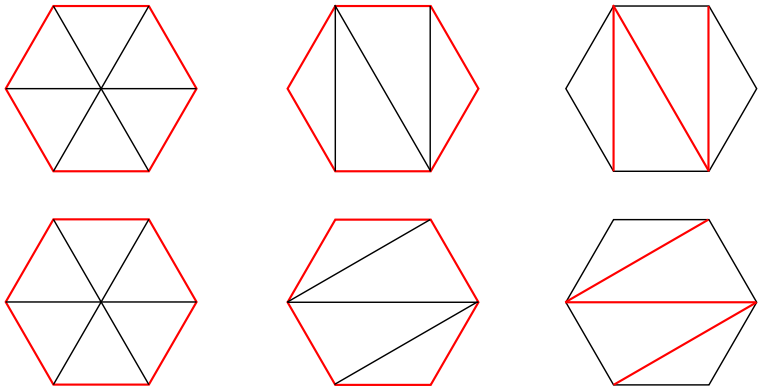

FIGURE 17. The singular fiber is the union of two ideal hexagons, each tessellated into 6 triangles (left). The regular fiber is also the union of two ideal hexagons, each tessellated into 4 ideal triangles (center). The surfaces are isotopic and are homeomorphic to a sphere with six punctures. At the next singular fiber, the surface is decomposed into two ideal hexagons in a different way, by cutting it along the new red edges (right). This shows the monodromy of the pseudo-Anosov fibration $M \to S^1$.

Proof. At the level $t = 0$, there are two octahedra O_0^{00} and O_0^{11} in $\widetilde{M}$. The two octahedra have opposite states, and thus they share the same closed red curve that separates the I faces from the O faces as in Figure 16-(right). This is the curve formed by the edges that have level $t = 0$. Each $C_0^{00} \subset O_0^{00}$ and $C_0^{11} \subset O_0^{11}$ is a cone (centered at the center of the octahedron) over this red curve, that is a pleated ideal hexagon, decomposed into six triangles. Each triangle has interior angles $\frac{\pi}{2}, 0, 0$. Two adjacent triangles meet at right angles. The intrinsic metric is that of a hexagon with a central conic point with angle 3π.

By Proposition 26 the singular fiber M^{sing} is isotopic to the union $C_0^{00} \cup C_1^{00}$, that is a sphere with six punctures, one at every cusp of M. Therefore the fiber of $M \to S^1$ is a sphere with six punctures.

We already know that the regular fiber M^{reg} is isotopic to the singular fiber, but we determine it anyway for a double check. By Proposition 26 the regular fiber is isotopic to the PL surface Σ that consists of all the ideal triangles that have level $t + \frac{1}{2}$. These are the four O faces of O_0^{00}, together with the four O faces of O_0^{11}. These correspond respectively to the four O and I faces of the ideal octahedron O. The forgetful map $\widetilde{M} \to O$ sends isometrically Σ to the boundary of O, which is again a sphere with 6 punctures. The regular fiber is isotopic to a sphere with six punctures Σ, tessellated into 8 ideal triangles. □

Figure 17 shows what goes on when we pass from a singular fiber to a regular fiber, and then to the next singular fiber of $\widetilde{M} \to \mathbb{R}$. The picture also displays the monodromy of the fiber that gives rise to the fibration $M \to S^1$. Recall that, since M is hyperbolic, the monodromy is pseudo-Anosov and hence no non-peripheral non-trival simple closed curve is preserved. We have here a reasonably simple description of a pseudo-Anosov monodromy.

4.3.3. *The ideal 24-cell.* Let $\mathcal{C} \subset \mathbb{H}^4$ be the ideal right-angled regular 24-cell coloured with three colours. We equip $\mathcal{C}$ wit the state s described in Section 3.3.3. We get a hyperbolic manifold W with 24 cusps and a Morse function $f\colon W \to S^1$ with 8 critical points of index 2, one at the center of each $\mathcal{C}^v$ as $v \in \mathbb{Z}_2^3$ varies. This is of course the manifold we are really interested in. We now determine the singular W^{sing} and the regular W^{reg} fibers. Quite unexpectedly, the singular fiber is quite special, because it is a cusped hyperbolic 3-manifold that decomposes into regular ideal tetrahedra (with four cusps coned).

Proposition 28. *The singular fiber W^{sing} is a cusped hyperbolic 3-manifold tessellated in 192 regular ideal tetrahedra with 28 cusps, four of which have been coned.*

Proof. At the level $t = 0$ there are four ideal 24-cells

$$\mathcal{C}_0^{000}, \quad \mathcal{C}_0^{011}, \quad \mathcal{C}_0^{110}, \quad \mathcal{C}_0^{101}.$$

With some patience we may check that the 48 ideal triangles in $\partial\mathcal{C}$ that separate the facets with status I from those with status O form a torus T with 24 punctures, one in each cusp of $\widetilde{W}$ (this is analogous to the red closed curve in the octahedron in Figure 16). The torus T is shown in Figure 18. Indeed the facets I and O form each a solid torus with 24 ideal vertices at the boundary. The cores of the two solid tori form a Hopf link in S^3, coherently with the descending and ascending links in the dual $\mathcal{C}^*$.

The configuration in each $\mathcal{C}_0^v$ is isometric to the one just described, but the position of the torus $T_0^v \subset \partial\mathcal{C}_0^v$ with 24 punctures (that consists of all the triangles in $\mathcal{C}_0^v$ with level 0) depends on v. By Proposition 26 the singular fiber is isotopic to the union

$$C_0^{000} \cup C_0^{011} \cup C_0^{110} \cup C_0^{101}$$

where C_0^v is the cone over T_0^v centered at the center of $\mathcal{C}_0^v$. Each C_0^v is tessellated into 48 tetrahedra. Therefore the singular fiber is decomposed into 192 tetrahedra. Each tetrahedron has three ideal vertices and one real one, the center of $\mathcal{C}_0^v$. The four centers of $\mathcal{C}_0^v$ are the singular points of the singular fiber W^{sing}.

By examining carefully the decomposition of the singular fiber into tetrahedra, we see that every face is adjacent to two tetrahedra (coherently with the fact that W^{sing} is singular only at the singular points) and more importantly every edge e

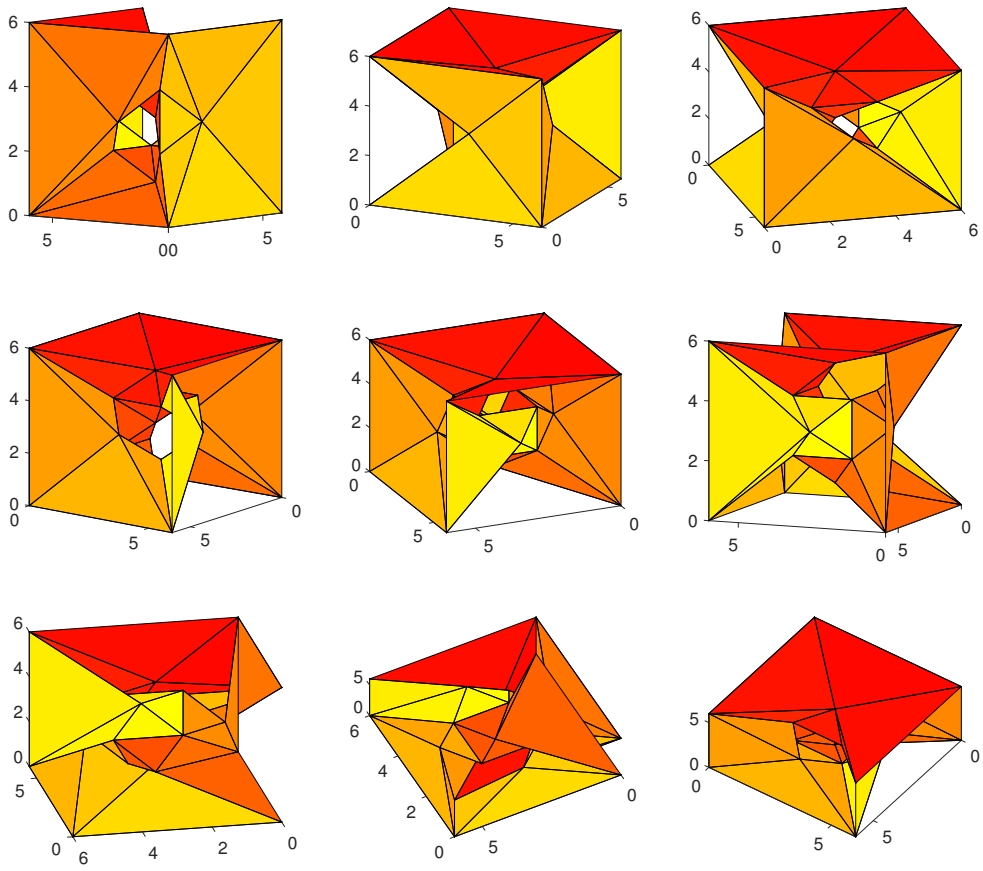

FIGURE 18. The triangles in the 2-skeleton of the 24-cell that separate facets with opposite IO status form a torus T, shown here from nine different viewpoints. In the pictures, we omit for the sake of clarity six triangles that are outside of the central cube and have a vertex at infinity. We may see that every vertex is adjacent to six triangles.

is adjacent to exactly 6 tetrahedra. This is due to the following facts, according to whether e is incident to a singular vertex or not, respectively:

(1) Every ideal vertex w of $\mathcal{C}_0^v$ is adjacent to 6 triangles of $\mathcal{C}_0^v$ of level 0 (this can be checked quite easily from Figure 9). Therefore the edge e connecting the center of $\mathcal{C}_0^v$ with w is adjacent to 6 tetrahedra.

(2) Every edge e of level $\frac{1}{2}$ is incident to three polytopes P_0^v of level 0, and inside each such polytope there are two tetrahedra incident to e. See Figure 15.

Given these premises, we can assign a hyperbolic metric to the singular manifold with its singular points removed by giving each tetrahedron the structure of an ideal regular tetrahedron in $\mathbb{H}^3$. □

We indicate with W^{sing} the singular fiber, and with $\mathring{W}^{\text{sing}} \subset W^{\text{sing}}$ the hyperbolic 3-manifold with 28 cusps. So W^{sing} is obtained by adding four points to $\mathring{W}^{\text{sing}}$. The surviving 24 cusps of W^{sing} are contained in the 24 cusps of W. The hyperbolic manifold $\mathring{W}^{\text{sing}}$ has volume ~ 194.868788.

It was expected that W^{sing} should have four singular points that are locally a cone over a torus, since this is what the critical fiber of a Morse function on a 4-manifold with index 2 looks like. This is coherent with the fact that $f\colon W \to S^1$ has eight critical points, because the singular fiber of f has two connected components, both diffeomorphic to W^{sing}, see Remark 25.

The fact that $\mathring{W}^{\text{sing}}$ is tessellated into ideal regular tetrahedra is quite special and is due to the extaordinary symmetries of $\mathcal{C}$, its colouring, and its state. We now turn to the regular fiber.

Proposition 29. *The regular fiber W^{reg} is a hyperbolic manifold tessellated into 48 (non regular) ideal octahedra. It is the double covering of the orbifold O shown in Figure 2. It has volume ~ 152.510077.*

Proof. The regular fiber W^{reg} decomposes into the 48 octahedral facets of level $\frac{1}{2}$. These are the 48 facets that have status O in some $\mathcal{C}_0^v$. The forgetful map $\pi\colon W^{\text{reg}} \to \partial\mathcal{C}$ is a branched covering of degree 2, since every facet of $\mathcal{C}$ has status O in two of the four polytopes $\mathcal{C}_0^v$ and status I in the other two.

Every edge e of $\mathcal{C}$ is adjacent to three facets, whose status can be OOO, OOI, OII, or III. We say that e is *even* or *odd* according to the parity of number of facets with status O incident to e. By a careful analysis we see that the branched covering π is ramified with index 2 along the even edges of $\mathcal{C}$, and that the even edges form the graph shown in Figure 2. From this we deduce that W^{reg} has 144 edges, 48 with valence 6 and 96 have valence 3. The valences 6 and 3 can also be inferred from Figure 15.

Using SnapPy we find that W^{reg} is hyperbolic and estimate its volume. In fact, we will later find that it is a cover of the hyperbolic manifold with one cusp `m036` from the census [8], so hyperbolicity is guaranteed. □

SnapPy tells us that both $\mathring{W}^{\text{sing}}$ and W^{reg} have plenty of isometries. This information has led us to study the isometries of $\widetilde{W}$ in the hope of finding some circle-valued Morse function on a smaller hyperbolic 4-dimensional manifold or orbifold, whose singular and regular fibers are some quotient of W^{sing} and W^{reg}.

5. Isometries and quotients

The circle-valued Morse function $W \to S^1$ of Theorem 2 is not difficult to describe, but we would like to find some smaller examples. We obtain these here by quotienting the covering manifold $\widetilde{W}$ by some appropriate group of symmetries.

The result of this quotient will be an orbifold Y and a circle-valued Morse function $f\colon Y \to S^1$ with some fibers Y^{sing} and Y^{reg} that are 48 times smaller than W^{sing} and W^{reg}.

5.1. **Isometries of $\mathcal{C}$.** The 24-cell has 1152 isometries. Half of these, that is 576, act orientation-preservingly. Every isometry of $\mathcal{C}$ preserves the partition of the facets of $\mathcal{C}$ into three B, R, and Y octets.

As we have seen in the proof of Proposition 21, left-multiplication by i refines this partition by subdividing each octet into two quartets. This refined partition into six quartets is *not* preserved by all the isometries of $\mathcal{C}$; only one third of them do: there are 192 orientation-preserving isometries that preserve the refined partition, and some of these will be considered below. These are particularly useful because they induce some isometry of $\widetilde{W}$, as we now see.

Let h be an isometry of $\mathcal{C}$ which preserves the refined partition into six quartets. The action on the partition induces an affine isomorphism $h_*\colon \mathbb{Z}_2^3 \to \mathbb{Z}_2^3$ as follows. Identify the colours B, R, Y with 1, 2, 3. Thus h acts on the set $\{1,2,3\}$. We define

$$h_*(v) = P(v+w) = P(v) + P(w)$$

where

- P is the permutation linear isomorphism determined by $P(e_i) = e_{h(i)}$,
- $w \in \mathbb{Z}_2^3$ is a fixed vector whose coordinates are $w_i = 1$ if h sends the facets coloured by i to those coloured by $h(i)$ by inverting their status, and $w_i = 0$ if they preserve it, for all $i = 1, 2, 3$.

The affine isomorphism h_* depends on how h acts on the colours and on the states of $\mathcal{C}$. We can check easily that $(h \circ h')_* = h_* \circ h'_*$ and $(h^{-1})_* = (h_*)^{-1}$. We also define $\varepsilon(h) = w_1 + w_2 + w_3 \in \mathbb{Z}_2$.

Proposition 30. *Every isometry h of $\mathcal{C}$ which preserves the refined partition into six quartets induces an isometry of $\widetilde{W}$ that sends $\mathcal{C}_t^v$ to $\mathcal{C}_{t+\varepsilon(h)}^{h_*(v)}$ via h.*

Proof. The isometry is well-defined, because it matches on every facet common to two adjacent 24-cells. This verification is left as an exercise. □

We have discovered as much as 192 isometries of $\widetilde{W}$ to play with. Half of them, that is 96, have $\varepsilon(h) = 0$, so they are level-preserving; they preserve the fibers $\widetilde{W}_t = \tilde{f}^{-1}(t)$ of $\tilde{f}\colon \widetilde{W} \to \mathbb{R}$ and form a finite group. We will see some concrete examples below.

5.2. **Some isometries of $\widetilde{W}$.** We now introduce some isometries of $\widetilde{W}$, many of which are derived from Proposition 30. We refer to the proof of Proposition 21 for some facts on quaternions and some notation. In particular we recall that the vertices of the dual 24-cell $\mathcal{C}^*$ form the group T^*_{24} and that the quartets are L_i-orbits. We note that left-multiplication by elements of Q_8 and right-multiplication by elements of T^*_{24} both (anti-)commute with L_i and hence preserve the refined partition into quartets. So by Proposition 30 all these isometries lift to $\widetilde{W}$.

5.2.1. *The isometry τ.* The monodromy τ of the covering map $\widetilde{W} \to W$ sends $\mathcal{C}^v_t$ to $\mathcal{C}^v_{t+2}$ via the identity map.

5.2.2. *The isometry ι.* The involution ι sends $\mathcal{C}^v_t$ to $\mathcal{C}^{v+e_1+e_2+e_3}_{1-t}$ via the identity map. It is well-defined because $\mathcal{C}^v$ and $\mathcal{C}^{v+e_1+e_2+e_3}$ have opposite states. It is orientation-reversing, and it induces an orientation-preserving isometry on the regular fiber $\widetilde{W}_{\frac{1}{2}}$, with fixed points the edges with level $\frac{1}{2}$.

The following examples are all derived from Proposition 30, applied to some left-multiplication by elements of Q_8 or right-multiplication by elements of T^*_{24}.

5.2.3. *The isometry L_i.* The left-multiplication L_i by i is an isometry of $\mathcal{C}$ that preserves both the colourings and the state. By acting as L_i on each $\mathcal{C}^v_t$ we get an isometry $L_i \colon \widetilde{W} \to \widetilde{W}$ of order 4.

5.2.4. *The isometry R_{z_0}.* The quaternion $z_0 = \frac{1}{2}(-1+i-j+k)$ is such that

$$1,\ z_0,\ z_0^2 = \frac{1}{2}(-1-i+j-k),\ z_0^3 = 1$$

are vertices of $\mathcal{C}^*$ with colour Y, R, B, Y and the same status I, I, I, I respectively, see Figures 9 and 10. The right-multiplication R_{z_0} by z_0 preserves the state of $\mathcal{C}$, while permuting the colours of the facets. By Proposition 30 we get a level-preserving isometry $R_{z_0} \colon \widetilde{W} \to \widetilde{W}$ of order 3 that sends $\mathcal{C}^v_t$ to $\mathcal{C}^{P(v)}_t$ via R_{z_0} where P is the permutation $P(v_1, v_2, v_3) = (v_2, v_3, v_1)$.

5.2.5. *The isometry S and the orbifold Q.* By composing the commuting isometries L_i and R_{z_0} of order 4 and 3 we get an isometry $S = L_i \circ R_{z_0}$ of $\mathcal{C}$ of order 12 that acts freely and transitively on the 12 facets with status O (and I) of $\mathcal{C}$. By definition

$$S(x) = ixz_0.$$

The quotient of $\mathcal{C}$ by this action is a hyperbolic 4-orbifold Q with one singular point that is locally a cone over the lens space $L(12,5)$,[1] and a boundary that consists of only two ideal regular octahedra with opposite status I and O, meeting at right angles (each octahedron is also self-adjacent along some triangular faces).

[1]There are only two lens spaces with π_1 of order 12, that is $L(12,1)$ and $L(12,5)$. Only the second decomposes into two octahedra (it decomposes geometrically into two regular spherical octahedra with angle $\frac{2\pi}{3}$). The first cannot be decomposed into two octahedra, because it cannot be decomposed with less than 9 tetrahedra [21]. So we are sure that the link is $L(12,5)$

We consider Q as a hyperbolic orbifold with right-angled cornered boundary. It has two ideal vertices with cubic link.

Proposition 30 furnishes a level-preserving isometry $S\colon \widetilde{W} \to \widetilde{W}$ of order 12 that sends $\mathcal{C}_t^v$ to $\mathcal{C}_t^{P(v)}$ via S where P is the permutation $P(v_1, v_2, v_3) = (v_2, v_3, v_1)$.

5.2.6. *The isometries L_j, L_k, R_i, R_j, R_k.* As we noted in the proof of Proposition 21, the isometries L_j, L_k preserve the colouring of $\mathcal{C}$ but invert the status IO of every facet, while R_i, R_j, R_k also preserves the colouring of $\mathcal{C}$ and inverts the status of every facet except those coloured as Y, B, or R respectively.

By Proposition 30, we get some isometries $L_j, R_i, R_j, R_k\colon \widetilde{W} \to \widetilde{W}$. The first sends $\mathcal{C}_t^v$ to $\mathcal{C}_{t+1}^{v+e_1+e_2+e_3}$ via L_j. The maps $R_i, R_j, R_k\colon \widetilde{W} \to \widetilde{W}$ send $\mathcal{C}_t^v$ to $\mathcal{C}_t^{v+e_1+e_2}$, $\mathcal{C}_t^{v+e_2+e_3}$, $\mathcal{C}_t^{v+e_3+e_1}$ via R_i, R_j, R_k respectively.

5.3. **The homology of $\widetilde{W}$.** We write $H_i(M)$ and $b_i(M)$ to denote the homology with real coefficients and its Betti numbers. We prove here the following:

Proposition 31. *The Betti numbers of $\widetilde{W}$ are*

$$b_1(\widetilde{W}) = 20, \qquad b_2(\widetilde{W}) = \infty, \qquad b_i(\widetilde{W}) = 0 \ \forall i \geq 3.$$

By Theorems 20 and 17 we know that the manifold $\widetilde{W}$ is obtained by $W^{\mathrm{reg}} \times [0,1]$ by attaching 2-handles. We recall a basic consequence of attaching a 2-handle to a manifold:

Lemma 32. *Let M be a manifold with boundary of dimension at least 2. Let N be a manifold obtained by attaching a 2-handle to M with core curve $\gamma \subset \partial M$. For $i \neq 1, 2$ we have $b_i(N) = b_i(M)$. For $i = 1, 2$ we have*

- *if γ is trivial in $H_1(M)$ then $b_1(N) = b_1(M)$ and $b_2(N) = b_2(M) + 1$;*
- *if γ is not trivial in $H_1(M)$ then $b_1(N) = b_1(M) - 1$ and $b_2(N) = b_2(M)$.*

Proof. Use Mayer-Vietoris. □

We calculate the Betti numbers of W^{reg} and W^{sing} via SnapPy or Sage, and get:

$$b_1(W^{\mathrm{reg}}) = 24, \qquad b_2(W^{\mathrm{reg}}) = 24, \qquad b_i(W^{\mathrm{reg}}) = 0 \ \forall i \geq 3;$$

$$b_1(W^{\mathrm{sing}}) = 20, \qquad b_2(W^{\mathrm{sing}}) = 24, \qquad b_i(W^{\mathrm{sing}}) = 0 \ \forall i \geq 3.$$

5.3.1. *The homology of $\widetilde{W}_{[\frac{1}{2}, \frac{3}{2}]}$.* The manifold $\widetilde{W}_{[\frac{1}{2}, \frac{3}{2}]}$ is obtained by thickening $\widetilde{W}_{\frac{1}{2}} \cong W^{\mathrm{reg}}$ and attaching four 2-handles along a multicurve α. It can also be obtained by thickening $\widetilde{W}_{\frac{3}{2}} \cong W^{\mathrm{reg}}$ and attaching four 2-handles along a multicurve γ (we will need this later). Furthermore, it deformation retracts onto W^{sing}, hence the Betti numbers of $\widetilde{W}_{[\frac{1}{2}, \frac{3}{2}]}$ are known.

5.3.2. *The homology of* $\widetilde{W}_{[-\frac{1}{2},\frac{3}{2}]}$. The manifold $X = \widetilde{W}_{[-\frac{1}{2},\frac{3}{2}]}$ is obtained by thickening $\widetilde{W}_{\frac{1}{2}} \cong W^{\mathrm{reg}}$ and attaching four 2-handles along a multicurve α on one boundary component, and four 2-handles along a multicurve β on the other boundary component. The isometry ι described in Subsection 5.2.2 preserves both $\widetilde{W}_{\frac{1}{2}}$ and $\widetilde{W}_{[-\frac{1}{2},\frac{3}{2}]}$, and interchanges the two multicurves α and β. Using Sage [31] we check that its induced isomorphism in homology

$$\iota_* : H_1(W^{\mathrm{reg}}) \to H_1(W^{\mathrm{reg}})$$

is the map $-\mathrm{Id}$. This implies that each curve in β is homologically trivial in $\widetilde{W}_{[\frac{1}{2},\frac{3}{2}]}$. Since X is obtained from $\widetilde{W}_{[\frac{1}{2},\frac{3}{2}]}$ by attaching handles along β, by Lemma 32 we get

$$b_1(X) = 20, \qquad b_2(X) = 28, \qquad b_i(X) = 0 \ \forall i \geq 3.$$

5.3.3. *The homology of* $\widetilde{W}_{[-\frac{1}{2}-n,\frac{3}{2}+n]}$. Recall that $\widetilde{W}_{[a,b]}$ and $\widetilde{W}_{[a+1,b+1]}$ are isometric, via the map L_j. So the arguments above apply in more generality, and show that for all $n \geq 1$, the manifold $\widetilde{W}_{[-\frac{1}{2}-n,\frac{3}{2}+n]}$ is obtained from $\widetilde{W}_{[\frac{1}{2}-n,\frac{1}{2}+n]}$ by attaching handles along homologically trivial multicurves. By Lemma 32 we get:

Theorem 33. *We have* $b_1(\widetilde{W}) = 20$, $b_2(\widetilde{W}) = \infty$, *and* $b_i(\widetilde{W}) = 0$ *for all* $i \geq 3$.

Corollary 34. *The fundamental group* $\pi_1(\widetilde{W})$ *is finitely generated but not finitely presented.*

Proof. Any finite set of generators for $\pi_1(W^{\mathrm{reg}})$ generate also $\pi_1(\widetilde{W})$. If $\pi_1(\widetilde{W})$ were finitely presented, then $H_2(\widetilde{W}) = H_2(\pi_1(\widetilde{W}))$ would be finitely generated. □

5.4. **A quotient.** Let $G < \mathrm{Isom}(\widetilde{W})$ be the group generated by the elements

$$G = \langle\ S,\ R_i,\ R_j,\ R_k\ \rangle.$$

The subgroups $\langle S \rangle$ and $\langle R_i, R_j, R_k \rangle$ have order 12 and 8, and they intersect in the group $\{L_{\pm 1}\} = \{R_{\pm 1}\}$ that has order 2. We can verify easily that G has order 48. Recall that $S^3 = L_{-i}$ and $S^4 = R_{z_0}$.

All the isometries in G are level-preserving (they form an index-2 subgroup of the level-preserving group of order 96 mentioned above). In particular they all preserve the fibers of $\tilde{f}\colon \widetilde{M} \to \mathbb{R}$. So by quotienting $\widetilde{W}$ via G we are quotienting the fibers.

Proposition 35. *The quotient* $\widetilde{Y} = \widetilde{W}/_G$ *is an orbifold that decomposes into copies* $Q_t, t \in \mathbb{Z}$ *of the orbifold with right-angled boundary* Q. *Each* Q_t *is adjacent to* Q_{t+1} *and* Q_{t-1} *along its octahedral facet with status O and I, respectively.*

The orbifold $\widetilde{Y}$ *has a singular point with link* $L(12,5)$ *at the center of each* Q_t, *and no other singular points. The number of strata that share the same level in* $\widetilde{W}$ *and* $\widetilde{Y}$ *is shown in Table 1.*

	4-strata	3-strata	2-strata	edges	cusps
$\widetilde{W}$	4 copies of $\mathcal{C}$	48 regular ideal octahedra	96 ideal triangles	48	24
$\widetilde{Y}$	1 copy of Q	1 regular ideal octahedron	2 ideal triangles	1	1

TABLE 1. The number and types of polytopes of each dimension with the same fixed level in $\widetilde{W}$ and $\widetilde{Y}$, and the number of cusps.

Proof. The four 24-cells $\mathcal{C}_t^v$ quotient to a single Q_t. With some patience we can show that the action of G on all the strata of dimension ≤ 3 is free. Therefore there are no other singular points and the numbers are those of Table 1. We also check that the action on the cusps is transitive, so they all quotient to a single one. □

The orbifold $\widetilde{Y}$ decomposes into an infinite row of copies of Q. The map $\tilde{f}\colon \widetilde{W} \to \mathbb{R}$ quotients to a map $\tilde{g}\colon \widetilde{Y} \to \mathbb{R}$. The singular W^{sing} and regular W^{reg} fibers quotient to some fibers of $\tilde{g}$ that we denote by Y^{sing} and Y^{reg}. The singular fiber Y^{sing} contains a singular point, the center of Q, and we let $\mathring{Y}^{\text{sing}}$ be Y^{sing} with the singular point removed. We have two regular coverings of degree 48

$$\mathring{W}^{\text{sing}} \longrightarrow \mathring{Y}^{\text{sing}}, \qquad W^{\text{reg}} \longrightarrow Y^{\text{reg}}.$$

By Propositions 28 and 29 both $\mathring{Y}^{\text{sing}}$ and Y^{reg} are cusped hyperbolic manifolds. Being 48 times smaller than $\mathring{W}^{\text{sing}}$ and W^{reg}, they can be found in the Callahan – Hildebrand – Weeks census [8] where they both have a name.

Proposition 36. *The fibers* $\mathring{Y}^{\text{sing}}$ *and* Y^{reg} *are* `m203` *and* `m036`*.*

Proof. The group G acts freely on the 192 regular ideal tetrahedra of $\mathring{W}^{\text{sing}}$ and on the 48 ideal regular octahedra of W^{reg}. Hence $\mathring{Y}^{\text{sing}}$ and Y^{reg} decompose into 4 regular ideal tetrahedra and 1 (non-regular) ideal octahedron.

With some patience we discover that the faces of the ideal octahedron in Y^{reg} are identified as shown in Figure 19. (This will be proved below in Proposition 37.) We can then give a triangulation to SnapPy and discover that $Y^{\text{reg}} =$ `m036`. In particular the manifold has only one cusp.

We know that $\mathring{Y}^{\text{sing}}$ has at least two cusps. The census [8] contains only two manifolds that decompose into 4 regular ideal tetrahedra with at least two cusps: these are `m202` and `m203`. They are respectively the Berge link and the 3/10 bridge-link exterior, see [22, page 1010].

By construction Y^{reg} must be a Dehn filling of $\mathring{Y}^{\text{sing}}$. Using SnapPy and [21] we see that `m036`, `m202`, and `m203` are all Dehn fillings of the magic manifold with coefficients respectively $(-\frac{1}{2}, -\frac{1}{2})$, $-\frac{5}{2}$, and $-\frac{1}{2}$. So in particular `m036` is a Dehn filling of `m203`. However, it cannot be a Dehn filling of `m202`, since [22, Table 2] shows that the

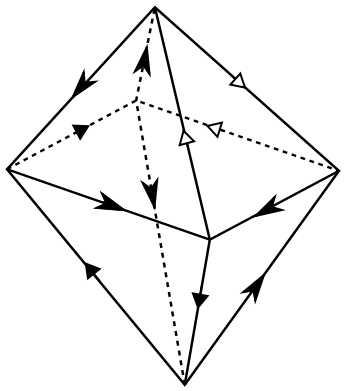

FIGURE 19. The manifold Y^{reg} is obtained by pairing the faces of the octahedron with the unique pair of isometries that match the arrows on the edges. The manifold so obtained has three edges with valence 3, 3, and 6.

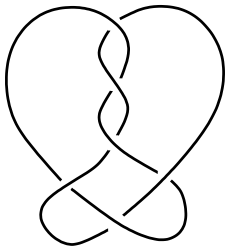

FIGURE 20. The link `L6a2` from Thistelthwaite link table. Its complement is `m203`.

Dehn filling $(-\frac{1}{2}, -\frac{1}{2}, -2)$ is the Seifert manifold $\big(S^2, (3,2), (3,-2), (3,-2)\big)$, which cannot be obtained from the Berge manifold `m202`, see [22, Tables 2, 3, 4]. □

The manifold `m203` is the complement of the link L6a2 from the Thistelthwaite link table, drawn in Figure 20. Using SnapPy we discover that its isometry group is isomorphic to the dihedral group D_8 of order 8. It acts transitively on the cusps, and faithfully on the homology $\mathbb{Z}^4$ of the boundary. It has an isometry that acts as $-I$ on the boundary homology, and hence trivially on the slopes. The group sends a pair (α, β) of slopes to (α, β), (β, α), $(-\alpha, -\beta)$, or $(-\beta, -\alpha)$. The manifold `m036` is obtained from `m203` by filling one boundary component with slope $\pm 3/2$. We note that the two slopes $3/2$ and $-3/2$ have distance 12.

The manifold `m036` has symmetry group $\mathbb{Z}_2 \times \mathbb{Z}_2$. Only one $\mathbb{Z}_2$ factor is induced by some isometry of `m203`. As we mentioned in the introduction, the manifold has one additional isometry that is not induced by `m203`, since it acts trivially on the homology $\mathbb{Z}^2$ of the boundary torus.

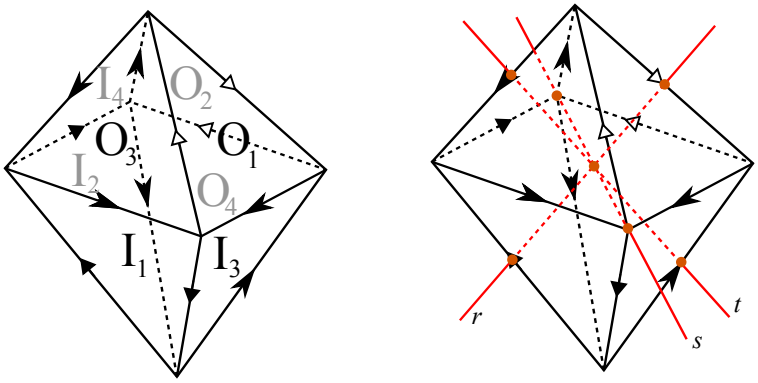

FIGURE 21. The facet with center $(1,0,0,0) \in \mathcal{C}^*$ and some axis of symmetries.

We may construct a quite small finite-volume hyperbolic 4-orbifold by setting

$$Y = \widetilde{Y}/_{\langle L_j \rangle}.$$

The orbifold Y contains a unique copy of Q. It has $\chi(Y) = \frac{1}{12}$. Its stratification consists simply of 1 copy of Q, 1 octahedron, 2 ideal triangles, and 1 edge. It has a unique singularity p, a cone over $L(12,5)$. The function $\widetilde{Y} \to \mathbb{R}$ descends to a circle-valued Morse function $Y \to S^1$ with a single critical point at p. We have proved Theorem 4.

5.5. **The representation.** We now describe explicitly the representation

$$\Phi \colon \pi_1(Y^{\mathrm{reg}}) \longrightarrow \mathrm{Isom}(\mathbb{H}^4) = O^+(4,1)$$

obtained by composing the homomorphism $i_* \colon \pi_1(Y^{\mathrm{reg}}) \to \pi_1(\widetilde{Y})$ induced by the inclusion $i \colon Y^{\mathrm{reg}} \hookrightarrow \widetilde{Y}$ and the holonomy injective representation $\pi_1(\widetilde{Y}) \to \mathrm{Isom}(\mathbb{H}^4)$.

Let us consider the octahedron of Figure 21. We denote by a, b, c, d the simplicial identifications of the faces:

$$a \colon O_1 \longrightarrow O_2, \quad b \colon I_1 \longrightarrow I_2, \quad c \colon O_3 \longrightarrow O_4, \quad d \colon I_3 \longrightarrow I_4$$

determined by the condition that edges with similar arrows in the figure must match.

Proposition 37. *The manifold Y^{reg} is obtained by quotienting the octahedron in Figure 21 via the identifications a, b, c, d. A presentation for $\pi_1(Y^{\mathrm{reg}})$ is*

$$\langle\, a, b \mid a^{-2}b^{-2}ab^{-2}a^{-2}b \,\rangle.$$

We have $c = a^2, d = b^2$, *and*

$$\Phi(a) = \begin{pmatrix} 1/2 & -1/2 & 1/2 & 1/2 & 0 \\ 1/2 & 1/2 & -1/2 & 1/2 & 0 \\ 1/2 & -1/2 & -1/2 & -1/2 & 0 \\ 1/2 & 1/2 & 1/2 & -1/2 & 0 \\ 0 & 0 & 0 & 0 & 1 \end{pmatrix},$$

$$\Phi(b) = \begin{pmatrix} -7/2 & 3/2 & 3/2 & 3/2 & 3\sqrt{2} \\ -3/2 & 1/2 & 1/2 & -1/2 & \sqrt{2} \\ 3/2 & 1/2 & -1/2 & -1/2 & -\sqrt{2} \\ 3/2 & -1/2 & 1/2 & -1/2 & -\sqrt{2} \\ -3\sqrt{2} & \sqrt{2} & \sqrt{2} & \sqrt{2} & 5 \end{pmatrix}.$$

Proof. We consider $\mathbb{H}^4 \subset \mathbb{R}^4$ with the Klein model, and the ideal regular 24-cell $\mathcal{C} \subset \mathbb{H}^4$ centered at the origin, positioned so that the vertices of the dual $\mathcal{C}^*$ (that correspond to the facets of $\mathcal{C}$) are the points in $\partial\mathbb{H}^4$ shown in Figure 9.

Let $F \subset \partial\mathcal{C}$ be the octahedral facet dual to the vertex $(1,0,0,0) \in \mathcal{C}^*$, that is the central yellow dot in Figure 9. The facet F has status O, see Figure 10. The triangular faces of F inherit the status I or O of the adjacent facets: we reproduce F in Figure 21-(left). The faces $I_1, \dots, O_4$ are adjacent to the facets that are dual to the following vertices of $\mathcal{C}^*$:

$$I_1 \to (+,-,-,-),\ I_2 \to (+,+,-,-),\ I_3 \to (+,-,-,+),\ I_4 \to (+,+,+,-),$$

$$O_1 \to (+,-,+,+),\ O_2 \to (+,+,+,+),\ O_3 \to (+,-,+,-),\ O_4 \to (+,+,-,+).$$

We identify $\mathcal{C}$ and $\mathcal{C}_0^0 \subset \widetilde{W}$. In the group G, the order-6 element S^2 acts on the facets of $\mathcal{C}$ as follows:

$$(+,-,+,-) \xrightarrow{S^2} (1,0,0,0) \xrightarrow{S^2} (+,+,-,+).$$

This implies that the face O_3 is identified to O_4, and by looking carefully at the action of S^2 we deduce that the identification is via the simplicial isomorphism c. Analogously by analysing S^7 we see that

$$(+,-,+,+) \xrightarrow{S^7} (1,0,0,0) \xrightarrow{S^7} (+,+,+,+).$$

Analogously, we deduce that the face O_1 is identified to O_2 via a. By writing S^7 in $O^+(4,1)$ we get the matrix $\Phi(a)$ shown above.

The isometry $\iota\colon \widetilde{W} \to \widetilde{W}$ described in Section 5.2.2 descends to an orientation-reversing isometric involution $\iota\colon \widetilde{Y} \to \widetilde{Y}$ that interchanges Q_0 and Q_1 and acts orientation-preservingly on Y^{reg}. To examine this action, we study the composition

$$\mathcal{C}_0^0 \xrightarrow{\iota} \mathcal{C}_1^{e_1+e_2+e_3} \xrightarrow{R_i} \mathcal{C}_1^{e_3}.$$

Recall that $R_i \in G$ and F separates $\mathcal{C}_0^0$ from $\mathcal{C}_1^{e_3}$. By looking at Figure 9 we deduce that $R_i \circ \iota$ preserves F and acts on it like a π-rotation around the axis s shown in

Figure 21-(right). Therefore ι lifts to a reflection $\iota\colon \mathbb{H}^4 \to \mathbb{H}^4$ around the axis line $s \subset F \subset \mathcal{C}_0^0 = \mathcal{C}$. The endpoints of s are the light vectors

$$(1, 1, 0, 0, \sqrt{2}), \qquad (1, -1, 0, 0, \sqrt{2}).$$

The reflection ι around s is then

$$\iota = \begin{pmatrix} -3 & 0 & 0 & 0 & 2\sqrt{2} \\ 0 & 1 & 0 & 0 & 0 \\ 0 & 0 & -1 & 0 & 0 \\ 0 & 0 & 0 & -1 & 0 \\ -2\sqrt{2} & 0 & 0 & 0 & 3 \end{pmatrix}.$$

We get the identifications b and d and their images $\Phi(b), \Phi(d)$ by conjugating a and c and their images $\Phi(a), \Phi(c)$ with ι. The presentation for $\pi_1(Y^{\mathrm{reg}})$ is then deduced from the edge of valence 6 in Figure 21-(left). □

The images of the two generators $\Phi(a)$ and $\Phi(b)$ are elliptic of order 12. As we have seen during the proof, they are conjugate along the isometric involution ι. The first homology of `m036` is $\mathbb{Z} \times \mathbb{Z}_3$.

Remark 38. The group G has index two in the level-preserving group of isometries of order 96 discussed in Section 5.1. By picking one lateral class we get one more level-preserving isometry ψ of $\widetilde{Y}$ that induces on Y^{reg} a π-rotation around the axis r shown in Figure 21. This isometry ψ is the one that is inherited by an isometry of `m203`. The composition $\iota \circ \psi = \psi \circ \iota$ induces a π-rotation along the axis t in the figure. The isometries $\{\mathrm{id}, \iota, \psi, \iota \circ \psi\}$ of $\widetilde{Y}$ form a group isomorphic to $\mathbb{Z}_2 \times \mathbb{Z}_2$. This is the full group of isometries of $Y^{\mathrm{reg}} =$ `m036`, as one sees using SnapPy. The isometries id and ψ are inherited from `m203`, but ι and $\iota \circ \psi$ are not.

5.6. **A simple self-contained description of Y.** As a consequence of the above discussion, we can describe Y concretely as a union of two four-dimensional hyperbolic pyramids with octahedral bases. Here are the details.

Let O be a facet of $\mathcal{C}$, that is a right-angled octahedron. Let v be the center of $\mathcal{C}$. We define P to be the cone over O with apex v. By construction $\mathcal{C}$ and Q decompose respectively into 24 and 2 copies of P.

The polytope P has a *base* O and eight *lateral facets*, those containing the apex v. It has 8 ideal vertices (those of O) and one real vertex v. The dihedral angles of P are $2\pi/3$ at the triangles containing v (the lateral ones), and $\pi/4$ at the triangles contained in O (the base ones).

Figure 22 shows two octahedra O_1 and O_2 and a face pairing giving $L(12, 5)$. Note that every edge has valence 3: if we give each O_i the structure of a spherical regular octahedron with dihedral angles $2\pi/3$, we get $L(12, 5)$ with its spherical metric.

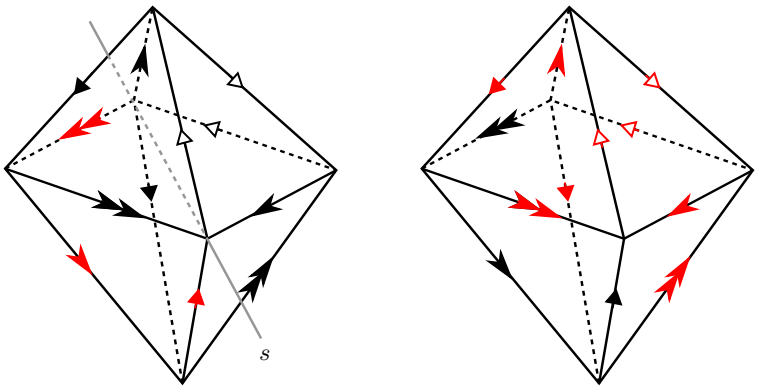

FIGURE 22. There is only one way to pair the faces of the two octahedra so that all the symbols at the edges match. The result is the lens space $L(12,5)$.

To get Q, just pick two copies P_1 and P_2 of P, and identify their lateral facets by extending the pairing shown in Figure 22 for their base octahedra O_1 and O_2. The link of v in Q is $L(12,5)$ decomposed as in the figure. (In fact, we found the figure by analysing carefully the link of Q.)

To get Y from Q, perform an additional identification by glueing the two octahedra O_1 and O_2 along the following isometry: first rotate O_1 of an angle π along the axis s shown in Figure 22, and then translate it to O_2. To verify that we get an orbifold Y with v as the only singular point, we just check that this identification produces two orbits of eight triangles, and since $8 \cdot \pi/4 = 2\pi$ we are done.

6. Infinitesimal rigidity of $\widetilde{W}$

We prove here the following.

Theorem 39. *The holonomy*

$$\rho : \pi_1(\widetilde{W}) \longrightarrow \mathrm{SO}^+(4,1)$$

of the hyperbolic structure on $\widetilde{W}$ is infinitesimally rigid.

6.1. **The space of infinitesimal deformations of a representation.** We recall some standard facts on deformations of hyperbolic structures. These can be found for instance in [19].

Let X be a hyperbolic manifold and ρ a representation of $\pi_1(X)$ in the Lie group $G = \mathrm{O}^+(4,1) = \mathrm{Isom}(\mathbb{H}^4)$. A *deformation* of ρ is a smooth path of representations ρ_t, with t varying in an interval $[0,\epsilon)$, such that $\rho_0 = \rho$. We can consider for each element g in $\pi_1(X)$ the initial deformation direction:

$$\frac{d}{dt}\rho_t(g)|_{t=0}.$$

In this way we assign to any element g of $\pi_1(X)$ a vector $\zeta(g)$ in the tangent space of $\rho(g)$ in G. From the Leibnitz rule we deduce the following equality

$$\zeta(gh) = \zeta(g)\rho(h) + \rho(g)\zeta(h).$$

In the literature the element $\zeta(g)$ is often moved to $\mathfrak{g}$ using the differential of the right-multiplication by $\rho(g)^{-1}$, that is itself the right multiplication by $\rho(g)^{-1}$ since G is a matrix group. So we define $z(g) = \zeta(g)\rho(g)^{-1}$ and obtain a map

$$z : \pi_1(X) \longrightarrow \mathfrak{g}.$$

To switch between ζ and z it is sufficient to right-multiply by $\rho(g)$ or by $\rho(g)^{-1}$. The Leibnitz rule for ζ transforms into the *cocycle condition*

$$z(gh) = z(g) + \rho(g)z(h)\rho(g)^{-1}.$$

A *cocycle* is a map $z\colon \pi_1(X) \to \mathfrak{g}$ that satisfies the cocycle condition. The cocycles form a vector space denoted by

$$Z^1(\pi_1(X), \mathfrak{g}_{\mathrm{Ad}\,\rho}). \tag{1}$$

This space contains the directions along which there is a chance to deform the representation ρ. Some of these directions are quite obvious and we would like to ignore them: consider a smooth path g_t of elements in G such that $g_0 = \mathrm{Id}$, and let k_t be the conjugation by the element g_t. It is possible to deform the representation ρ as $\rho_t = k_t(\rho)$. The resulting deformation direction z only depends on the tangent vector $V = \frac{d}{dt}g_t|_{t=0} \in \mathfrak{g}$. Explicitly, we get

$$\zeta(g) = V\rho(g) - \rho(g)V, \qquad z(g) = V - \rho(g)V\rho(g)^{-1}.$$

A cocycle obtained in this way is called a *coboundary*, and the subspace of all coboundaries is denoted by $B^1(\pi_1(X), \mathfrak{g}_{\mathrm{Ad}\,\rho})$. The quotient of these two spaces

$$H^1(\pi_1(X), \mathfrak{g}_{\mathrm{Ad}\,\rho}) = \frac{Z^1(\pi_1(X), \mathfrak{g}_{\mathrm{Ad}\,\rho})}{B^1(\pi_1(X), \mathfrak{g}_{\mathrm{Ad}\,\rho})}$$

is called the *space of infinitesimal deformations* of ρ. We say that ρ is *infinitesimally rigid* if such space is trivial.

This definition gains importance under the light of Weil's lemma [29], that asserts that any infinitesimally rigid representation is also *locally rigid*, that is any deformation of ρ is induced by a path of conjugations. If ρ is the holonomy of a complete hyperbolic structure, this in turn implies that the hyperbolic structure of X cannot be deformed.

Remark 40. The cocycle condition implies the following:

$$z(g^{-1}) = -\rho(g)^{-1}z(g)\rho(g), \qquad z(e) = 0.$$

By construction we have a surjective homomorphism

$$\psi\colon \mathfrak{g} \longrightarrow B^1(\pi_1(X), \mathfrak{g}_{\mathrm{Ad}\,\rho}), \qquad \psi(V)(g) = V\rho(g) - \rho(g)V.$$

Proposition 41. *If the image of ρ has limit set $S^3 = \partial\mathbb{H}^4$, the map ψ is an isomorphism.*

Proof. If ψ were not injective, we would get a non-trivial matrix $V \in \mathfrak{g}$ that commutes with the image of ρ. Therefore $e^V \in G = \mathrm{Isom}(\mathbb{H}^4)$ would be a non-trivial isometry that commutes with the image of ρ. This is easily seen to be impossible when the limit set is S^3. □

Corollary 42. *With the same hypothesis, we get*

$$\dim B^1(\pi_1(X), \mathfrak{g}_{\mathrm{Ad}\,\rho}) = \dim \mathfrak{g} = \dim G = 10.$$

6.2. **Finitely presented groups.** If $\pi_1(X)$ is finitely presented, we can determine $H^1(\pi_1(X), \mathfrak{g}_{\mathrm{Ad}\,\rho})$ as follows. Given a finite presentation

$$\pi_1(X) = \langle\, g_1, \dots, g_h \mid r_1, \dots, r_k \,\rangle,$$

and a representation $\rho\colon \pi_1(X) \to G$, a deformation of ρ is of course determined by its behaviour on the generators. The same holds for a cocycle z in $Z^1(\pi_1(X), \mathfrak{g}_{\mathrm{Ad}\,\rho})$ since the following equalities hold

$$z(gh) = z(g) + \rho(g)z(h)\rho(g)^{-1}, \qquad z(g^{-1}) = -\rho(g)^{-1}z(g)\rho(g).$$

In particular $H^1(\pi_1(X), \mathfrak{g}_{\mathrm{Ad}\,\rho})$ has finite dimension. An arbitrary assignment of elements in $\mathfrak{g}$ to the generators of $\pi_1(X)$ will not give rise to a cocycle in general: this assignment must fulfill some requirements that we now describe.

We represent the cocycles using ζ instead of z. We get

$$\zeta(gh) = \zeta(g)\rho(h) + \rho(g)\zeta(h), \qquad \zeta(g^{-1}) = -\rho(g)^{-1}\zeta(g)\rho(g)^{-1}. \tag{2}$$

Given a word w in $g_1, \dots, g_h$ and their inverses and some invertible matrices $A_1, \dots, A_h$, we denote by $w(A_1, \dots, A_h)$ the matrix obtained by substituting in w each g_j with A_j. Consider a h-uple of matrices

$$D = (D_1, \dots, D_h) \in (M(5, \mathbb{R}))^h.$$

Proposition 43. *There is a cocyle ζ with $\zeta(g_i) = D_i$ for all i if and only if:*

- *every element D_i is in the tangent space in G at $M_i = \rho(g_i)$, and*
- *the relations vanish at first order along the direction D,* i.e.

$$\frac{d}{dt} r_i(M_1 + tD_1, \dots, M_h + tD_h)\Big|_{t=0} = 0 \quad \forall i = 1, \dots, k. \tag{3}$$

In this case we have

$$\zeta(g) = \frac{d}{dt} w(M_1 + tD_1, \dots, M_h + tD_h)\Big|_{t=0} \tag{4}$$

for every word w that represents g.

Proof. Let $D_1, \dots, D_h$ satisfy both conditions. We define $\zeta(g)$ using (4). The definition is well-posed: indeed, if for every word w we define

$$\zeta(w) = \frac{d}{dt} w(M_1 + tD_1, \dots, M_h + tD_h)\Big|_{t=0}$$

then we easily deduce from the Leibnitz rule that

$$\zeta(w_1 w_2) = \zeta(w_1)\rho(w_2) + \rho(w_1)\zeta(w_2), \qquad \zeta(w^{-1}) = -\rho(w)^{-1}\zeta(w)\rho(w)^{-1}.$$

By hypothesis $\zeta(r_i) = 0$ and of course $\rho(r_i) = I$. This implies easily that ζ vanishes on every word obtained from the relators by conjugations, products, and inverses. This in turn easily implies that $\zeta(w_1) = \zeta(w_2)$ whenever two words w_1 and w_2 indicate the same element g of the group.

Conversely, let ζ be a cocycle. We first prove (4). The equality holds when $w = g_i$, and we deduce easily that it holds for any word w using (2). We then deduce (3) using $w = r_i$. □

We can view a cocycle ζ as an assignment of matrices $D_1, \dots, D_h$ to the generators $g_1, \dots, g_h$ that fulfill some requirements. A coboundary is determined by a vector $V \in \mathfrak{g}$ as $\zeta(g) = V\rho(g) - \rho(g)V$. We may pick a basis for $\mathfrak{g}$ and get a finite set of generators for $B^1(\pi_1(X), \mathfrak{g}_{\mathrm{Ad}\,\rho})$.

6.3. **Fundamental groupoids.** The theory introduced in the previous pages extends from fundamental groups to fundamental groupoids with roughly no variation. This extension will be useful for us to prove Theorem 39.

Let X be a path-connected topological space and $V \subset X$ a finite set of points. The *fundamental groupoid* $\pi_1(X, V)$ relative to V is the the set of continuous maps $\alpha : [0, 1] \to X$ with extremal points in V, up to homotopy which fixes the extremal points. It is possible to concatenate two such paths if the ending point of the first is the initial point of the second. When we write $\alpha_2\alpha_1$ we mean that the first path is α_1 and the second one is α_2, and concatenation is possibile.

The fundamental groupoid has a trivial element e_v for every $v \in V$. For every $v \in V$, the inclusion defines an injection $i_* \colon \pi_1(X, v) \hookrightarrow \pi_1(X, V)$.

A *finite presentation* of a groupoid is defined in the same way as for groups, as a set of generators and relators

$$\langle\ g_1, \dots, g_h \mid r_1, \dots, r_k\ \rangle$$

where each g_i is an element of the groupoid, each r_j is a word in the $g_i^{\pm 1}$ that represents some trivial element, every element of the groupoid is represented as a word in the $g_i^{\pm 1}$, and two words w_1, w_2 represent the same element if and only if $w_1 w_2^{-1}$ makes sense and is obtained from the relations by formal conjugations, inversions, and multiplications.

Let $V = \{v_0, \dots, v_s\}$. For every $i = 1, \dots, s$ pick an arc α_i connecting v_0 and v_i. Given a finite presentation $\langle\ g_i \mid r_j\ \rangle$ for $\pi_1(X, v_0)$, we can construct one for $\pi_1(X, V)$ by adding the arcs $\alpha_1, \dots, \alpha_s$ as generators.

We will always suppose that $\pi_1(X, V)$ has a finite presentation.

6.4. **Representations and cocycles.** A *groupoid representation* is a map

$$\sigma : \pi_1(X, V) \to G$$

such that $\sigma(\beta\alpha) = \sigma(\beta)\sigma(\alpha)$ whenever it is possible to concatenate α and β. (Usually, a groupoid representation assigns a vector space to each $v \in V$ and sends elements to morphisms between these vectors spaces: here we simply assign the same vector space $\mathbb{R}^5$ to every v and require the morphisms to lie in $G = O^+(4, 1)$.)

Given a grupoid representation σ, it is possible to define its deformations and the cocycles as we did in the previous section, the only difference being that multiplications should be considered only when they make sense.

A cocycle z is a map $z\colon \pi_1(X, V) \to \mathfrak{g}$ that fulfills the cocycle condition (1) for every pair $g, h \in \pi_1(X, V)$ of elements that can be multiplied. We denote the vector space of all cocycles as $Z^1(\pi_1(X, V), \mathfrak{g}_{\mathrm{Ad}\,\sigma})$. We still have two versions z and ζ of the same cocycle that differ only by right multiplication by $\sigma(g)^{-1}$. As in the previous case a coboundary is determined by a vector $V \in \mathfrak{g}$ as $\zeta(g) = V\rho(g) - \rho(g)V$ and the subspace of all coboundaries is denoted by $B^1(\pi_1(X, V), \mathfrak{g}_{\mathrm{Ad}\,\sigma})$. The quotient of these two spaces is $H^1(\pi_1(X, V), \mathfrak{g}_{\mathrm{Ad}\,\sigma})$.

Proposition 43 is still valid in this context, with the same proof. If we have a finite presentation of $\pi_1(X, V)$, we can determine all the cocycles in $H^1(\pi_1(X, V), \mathfrak{g}_{\mathrm{Ad}\,\sigma})$ in their ζ version by assigning some matrices D_i to the generators that fulfill the indicated requirements at the relators.

The representation σ induces a representation $\rho = \sigma \circ i_*$ for $\pi_1(X, v_0)$. The spaces $Z^1(\pi_1(X, V), \mathfrak{g}_{\mathrm{Ad}\,\sigma})$ and $Z^1(\pi_1(X, v_0), \mathfrak{g}_{\mathrm{Ad}\,\rho})$ are related in a simple way:

Proposition 44. *The inclusion i induces a surjective map*

$$i^*\colon Z^1(\pi_1(X, V), \mathfrak{g}_{\mathrm{Ad}\,\sigma}) \longrightarrow Z^1(\pi_1(X, v_0), \mathfrak{g}_{\mathrm{Ad}\,\rho}).$$

The dimension of its kernel is $\dim(G) \cdot (|V| - 1)$.

Proof. Pick a finite presentation $\langle\ g_i \mid r_j\ \rangle$ for $\pi_1(X, v_0)$ and some arcs α_k connecting v_0 to v_k. Then $\langle\ g_i, \alpha_k \mid r_j\ \rangle$ is a presentation for $\pi_1(X, V)$. A cocycle ζ for ρ extends to a cocycle ζ' for σ by assigning to each α_k and arbitrary matrix tangent to G in $\sigma(\alpha_k)$. The resulting ζ' is a cocycle by Proposition 43, since both presentations have the same relators. There are $|V| - 1$ arcs α_k and a space of dimension $\dim(G)$ to choose from for each arc. □

The proposition can be upgraded for the representation ρ we are interested in.

Corollary 45. *If the image of ρ has limit set S^3, the inclusion i induces a surjective homomorphism*

$$i^*\colon H^1(\pi_1(X,V),\mathfrak{g}_{\mathrm{Ad}\,\sigma}) \longrightarrow H^1(\pi_1(X,v_0),\mathfrak{g}_{\mathrm{Ad}\,\rho}).$$

The dimension of its kernel is $\dim(G)\cdot(|V|-1)$.

Proof. The spaces $B^1(\pi_1(X,V),\mathfrak{g}_{\mathrm{Ad}\,\sigma})$ and $B^1(\pi_1(X,v_0),\mathfrak{g}_{\mathrm{Ad}\,\rho})$ have both dimension equal to $\dim G = 10$ by Proposition 41. Hence the map i^* sends the former to the latter isomorphically. □

6.5. **Cube complexes.** Let C be a finite connected cube complex. It is natural here to consider its set of vertices V and the fundamental groupoid $\pi_1(C,V)$. This has a natural presentation

$$\langle\ g_1,\dots,g_h \mid r_1,\dots,r_k\ \rangle \tag{5}$$

where $g_1,\dots,g_h$ are the edges of C, oriented arbitrarily, and $r_1,\dots,r_k$ are 4-letters words in the $g_i^{\pm1}$ arising from the square faces of C, oriented arbitrarily.

Let v be a fixed vertex of C. To pass from the presentation (5) of $\pi_1(C,V)$ to one for the fundamental group $\pi_1(C,v)$ it suffices to choose a maximal tree T in the 1-skeleton of C and to add a relator g_i representing every edge contained in T.

6.6. **The rigidity of $\widetilde{W}$.** We are now ready to prove Theorem 39. The holonomy of $\widetilde{W}$ is a homomorphism

$$\rho : \pi_1(\widetilde{W}) \longrightarrow \mathrm{Isom}(\mathbb{H}^4).$$

The manifold $\widetilde{W}$ deformation retracts onto the infinite cube complex C, see Subsection 1.3. The fundamental group $\pi_1(\widetilde{W})$ is not finitely presented and C is infinite, so the techniques introduced in the previous section do not apply here. However, it will be sufficient to consider a finite portion C' of C and use the following.

Proposition 46. *Let C' be a finite subcomplex of C such that*

$$i_*\colon \pi_1(C',v_0) \twoheadrightarrow \pi_1(C,v_0)$$

is surjective. If $\rho' = \rho\circ i_*$ is infinitesimally rigid then ρ is infinitesimally rigid.

Proof. The surjective homomorphism i_* induces an injective homomorphism

$$i^*\colon H^1(\pi_1(C,v_0),\mathfrak{g}_{\mathrm{Ad}\,\rho}) \longrightarrow H^1(\pi_1(C',v_0),\mathfrak{g}_{\mathrm{Ad}\,\rho\circ i_*}).$$

If the target space is trivial, the domain also is. □

Recall that every k-cube of C has some level. We now define a finite subcomplex $C'\subset C$ as the full subcomplex that is generated by all the vertices of level $-1,0,1$. This consists of these vertices, of all the edges of level $\pm1/2$, and of all the squares of level 0. In other words C' is the smallest subcomplex that contains all the squares of level 0. The subcomplex C' has 12 vertices, 96 edges, and 96 squares.

It is connected, and the inclusion $C' \hookrightarrow C$ is π_1-surjective because it contains the 1-skeleton of $\widetilde{W}_0 \cong \widetilde{W}^{\mathrm{sing}}$. We will prove that the representation $\rho' = \rho \circ i_*$ is infinitesimally rigid.

Let V (respectively, V') be the set of vertices of C (respecively, C'). The representation ρ (respectively, ρ') extends to a representation σ (respectively, σ') of the groupoid $\pi_1(C, V)$ (respectively, $\pi_1(C', V')$) that is easy to describe. Consider the orbifold-covering

$$p : \widetilde{W} \longrightarrow \mathcal{C}$$

where $\mathcal{C}$ is the 24-cell, interpreted as an orbifold $\mathcal{C} = \mathbb{H}^4/_\Gamma$. Here Γ is the Coxeter group generated by reflections along the facets of $\mathcal{C}$. The map p sends every vertex of V to the center v of $\mathcal{C}$. It induces a map

$$p_* : \pi_1(C, V) \longrightarrow \pi_1(\mathcal{C}, v) = \Gamma.$$

Consider the natural presentation $\langle\, g_i \mid r_j \,\rangle$ of $\pi_1(C, V)$, with generators and relators corresponding to oriented edges and squares of C. Every g_i corresponds to an oriented edge of C, which in turn determines a facet F of $\mathcal{C}$. The map p_* sends g_i to the reflection r_F along F. The orientation of g_i is not important since $r_F^2 = \mathrm{id}$.

The map p_* is very convenient because it sends every generator g_i to a reflection r_F. We write $\sigma = p_*$ and denote by σ' its restriction to $\pi_1(C', V')$.

We now need to calculate the dimension of $H^1(\pi_1(C', V'), \mathfrak{g}_{\mathrm{Ad}\,\sigma'})$. To do this we create a linear system and we study its solutions using MATLAB.

6.6.1. *The algorithm.* In this subsection we briefly explain the algorithm that we used to build up and solve our linear system. The code can be found at [31].

We write a Python code that enumerates the 96 edges of C', noticing that these are in 1-1 correspondence with the edges of the cube complex associated to W, the manifold made up by eight 24-cells covered by $\widetilde{W}$. We orient each edge from the vertex of level 0 towards the other vertex, which has level ± 1. The 96 edges represent the 96 generators of $\pi_1(C', V)$. Each generator g_i is sent by σ' to a reflection r_F along a facet F of $\mathcal{C}$, that we denote by M_i to be consistent with Proposition 43.

Then we need to encode the 96 squares of level 0. These correspond dually to the 96 triangular faces of the four 24-cells of level 0 that separate the facets with different IO status. Once we have a list of them we orient them arbitrarily.

We can now write our linear system with MATLAB. We have a deformation D_i for every generator g_i, and this gives $96 \cdot 25 = 2400$ variables, since D_i is an unknown 5×5 matrix. Following Proposition 43, the deformations have to fulfill two types of linear equations:

- they must lie in the tangent space at M_i. This is achieved by imposing the equation

$$D_i^t \cdot J \cdot M_i + (J \cdot M_i)^t \cdot D_i = 0,$$

where $J = \mathrm{diag}(1, 1, 1, 1, -1)$;

- they have to solve the equations given by the relations. We have one equation for each square in C'.

Using MATLAB we discover that the solution space for this linear system has dimension 120. Therefore

$$\dim Z^1(\pi_1(C', V'), \mathfrak{g}_{\mathrm{Ad}\,\sigma'}) = 120.$$

Since V' consists of 12 vertices, Proposition 44 tells us that

$$\dim Z^1(\pi_1(C', v_0), \mathfrak{g}_{\mathrm{Ad}\,\rho'}) = 10.$$

Finally, Corollary 42 tells us that $H^1(\pi_1(C', v_0), \mathfrak{g}_{\mathrm{Ad}\,\rho'})$ is trivial. The representation ρ' is infinitesimally rigid, and hence ρ also is by Proposition 46.

The proof of Theorem 39 is complete.

References

[1] I. Agol, *The virtual Haken conjecture* (with an appendix by I. Agol, D. Groves and J. Manning), Doc. Math. **18** (2013), 1045–1087.

[2] I. Agol – M. Stover, *Congruence RFRS towers*, `arXiv:1912.10283`

[3] M. Bell, *Recognising Mapping Classes*, PhD thesis.

[4] M. Bestvina – N. Brady, *Morse theory and finiteness properties of groups*, Invent. Math., **129** (1997), 445–470.

[5] S. Bleiler – C. Hodgson – J. Weeks, *Cosmetic surgery on knots*, in "Proceedings of the Kirbyfest" (Berkeley, CA, 1998), 23–34 (electronic), Geometry and Topology Monographs, **2**, Coventry, 19.

[6] J. Brock – K. Bromberg, *On the density of geometrically finite Kleinian groups*. Acta Math., **192** (2004), 33–93.

[7] K. Bromberg, *Projective structures with degenerate holonomy and the Bers density conjecture*, Ann. of Math. **166** (2007), 77–93.

[8] P. Callahan – M. Hildebrand – J. Weeks, *A census of cusped hyperbolic 3-manifolds*, Math. Comp. **68** (1999), 321–332.

[9] M. Culler – N. Dunfield – M. Görner – J. Weeks, *SnapPy, a computer program for studying the geometry and topology of 3-manifolds*, `http://www.math.uic.edu/t3m/SnapPy/`

[10] S. Friedl – S. Vidussi, *Virtual algebraic fibrations of Kähler groups*, `arXiv:1704.07041`, to appear in Nagoya Math. J.

[11] D. Heard – E. Pervova – C. Petronio, *The 191 orientable octahedral manifolds*. Experiment. Math., **17** (2008), 473–486.

[12] M. W. Hirsch – B. Mazur, "Smoothings of piecewise linear manifolds," Princeton University Press, Princeton, NJ, 1974, Annals of Mathematics Studies, No. 80.

[13] G. Italiano – B. Martelli – M. Migliorini, *Hyperbolic manifolds that fiber algebraically up to dimension 8*, preprint.

[14] K. Jankiewicz – S. Norin – D. T. Wise, *Virtually fibering right-angled Coxeter groups*, to appear in J. Inst. Math. Jussieu.

[15] T. Jørgensen, *Compact 3-manifolds of constant negative curvature fibering over the circle*, Ann. Math. **106** (1977), 61–72.

[16] M. Kapovich, *On the absence of Sullivan's cusp finiteness theorem in higher dimensions*, in "Algebra and analysis" (Irkutsk, 1989), Amer. Math. Soc., Providence, RI, 1995, pp. 77–89.

[17] ———, *Kleinian groups in higher dimensions*, Geometry and dynamics of groups and spaces, 487–564, Progr. Math., **265**, Birkhuser, Basel, 2008.

[18] D. Kielak, *Residually finite rationally-solvable groups and virtual fibring*. `arXiv:1809.09386`, To appear in J. Amer. Math. Soc.

[19] S. Kerckhoff – P. Storm, *Local rigidity of hyperbolic manifolds with geodesic boundary*. J. Topol., **5** (2012), 757–784.

[20] A. Kolpakov – B. Martelli, *Hyperbolic four-manifolds with one cusp*, Geom. & Funct. Anal. **23** (2013), 1903–1933.

[21] B. Martelli – C. Petronio, *Three-manifolds having complexity at most 9*, Experiment. Math. **10** (2001), 207–237.

[22] ———, *Dehn filling of the "magic" 3-manifold*, Comm. Anal. Geom. **14** (2006), 969–1026.

[23] B. Martelli – S. Riolo, *Hyperbolic Dehn filling in dimension four*, Geom. & Topol. **22** (2018), 1647–1716.

[24] Y. Minsky, *The classification of Kleinian surface groups, I: Models and bounds*, Ann. of Math. **171** (2010), 1–107.

[25] J. R. Munkres, *Obstructions to the smoothing of piecewise-differentiable homeomorphisms*, Ann. of Math. (2) **72** (1960), 521–554.

[26] H. Namazi – J. Souto, *Non-realizability and ending laminations: Proof of the density conjecture*, Acta Math., **209** (2012), 323–395.

[27] C. Rourke – B. Sanderson, "Introduction to piecewise-linear topology," Springer–Verlag 1972.

[28] H.C. Wang *Topics on totally discontinuous groups*, Symmetric Spaces, W.M. Boothby and G.L. Weiss, eds, Pore Appl. Math. **8**, Marcel Dekker, New York (1972), 459–487.

[29] A. Weil, *Remarks on the cohomology of groups*, Ann. of Math. **80** (1964), 149–157.

[30] D. T. Wise, *The structure of groups with a quasi-convex hierarchy*, preprint. Available at `http://www.math.mcgill.ca/wise/papers`

[31] `http://people.dm.unipi.it/battista/code/geom_inf_rigid_4_manifold/`